

# A geospatial model of ambient sound pressure levels in the contiguous United States

Daniel Mennitt,<sup>a)</sup> Kirk Sherrill, and Kurt Fristrup

Natural Sounds and Night Skies Division, National Park Service, 1201 Oakridge Drive, Suite 100,  
Fort Collins, Colorado 80525

(Received 21 March 2013; revised 2 October 2013; accepted 21 March 2014)

This paper presents a model that predicts measured sound pressure levels using geospatial features such as topography, climate, hydrology, and anthropogenic activity. The model utilizes *RANDOM FOREST*, a tree-based machine learning algorithm, which does not incorporate *a priori* knowledge of source characteristics or propagation mechanics. The response data encompasses 270 000 h of acoustical measurements from 190 sites located in National Parks across the contiguous United States. The explanatory variables were derived from national geospatial data layers and cross validation procedures were used to evaluate model performance and identify variables with predictive power. Using the model, the effects of individual explanatory variables on sound pressure level were isolated and quantified to reveal systematic trends across environmental gradients. Model performance varies by the acoustical metric of interest; the seasonal  $L_{50}$  can be predicted with a median absolute deviation of approximately 3 dB. The primary application for this model is to generalize point measurements to maps expressing spatial variation in ambient sound levels. An example of this mapping capability is presented for Zion National Park and Cedar Breaks National Monument in southwestern Utah.

© 2014 Acoustical Society of America. [<http://dx.doi.org/10.1121/1.4870481>]

PACS number(s): 43.50.Rq, 43.28.Js, 43.28.Hr, 43.50.Vt [SF]

Pages: 2746–2764

## I. INTRODUCTION

The atmospheric environment is filled with sounds that vary in number, structure, and magnitude across time and space. Natural phenomena such as time of day, seasonality, location, terrain, weather, temperature, and animal distribution and behavior influence the structure and complexity of the natural acoustical environment.<sup>1–3</sup> For example, there are more than a thousand species of grasshoppers, crickets, and other Orthoptera in North America. Each species of this soniferous order contributes a unique voice to the natural chorus, a voice modulated by season, time of day, and temperature. The wealth of ecological information revealed by natural sounds—as well as the high public value placed on soundscape preservation—has motivated diverse efforts to measure, understand, and manage acoustical environments.<sup>4–14</sup>

The U. S. Congress required the National Park Service (NPS) to focus on acoustic resource conservation in 1975 identifying “natural quiet” as a resource and a value to be protected in Grand Canyon (Public Law 93–620). Since then, over 250 000 h of acoustical monitoring data have been collected from hundreds of sites in NPS units.<sup>4</sup> These extensive data, acquired at substantial cost, represent an extremely sparse spatial sample of the  $34 \times 10^6$  hectares of land and 730 000 hectares of aquatic habitats managed by the NPS. These site data can be generalized into maps of predicted sound levels, with accompanying estimates of predictive accuracy, by determining the relationships between measured

sound levels and geospatial data sets having continental coverage. The resulting maps will clarify the range of resource conditions within park units, and support resource management across regional scales and multiple management authorities.<sup>15</sup> This approach parallels a proposal by Ferrier for addressing gaps in spatial monitoring of biodiversity.<sup>16</sup>

This paper presents a model relating expected sound pressure levels to geospatial data quantifying biological, geophysical, climatic, and anthropogenic variables. The measurements that are predicted are long term seasonal values of one-third octave band levels and full spectrum weighted and unweighted levels. Finer time scales are not addressed. Numerous approaches to regression analysis exist, each with affinities for particular data sets. Machine learning methods are desirable in situations where the form of the dependency between variables is unknown, or if a given variable has any predictive power at all. In this paper, relationships between the acoustic and geospatial data were discovered using *RANDOM FOREST*, a tree-based machine learning algorithm.<sup>17</sup> Section II introduces the acoustic and geospatial data sets used to train the models in more detail. Section III presents an overview of the *RANDOM FOREST* algorithm and the methods used for construction and evaluation of the geospatial model. Results of the modeling effort show that non-acoustic geospatial information can help predict sound pressure levels. These explanatory variables have been identified using a method that imposes a strict criterion based on exhaustive leave-one-out cross validation error. The collective structure of the measured soundscapes is discussed in Sec. IV. The influence of important explanatory variables on sound pressure level was quantified. The relative contributions across the spectrum show how geospatial

<sup>a)</sup>Author to whom correspondence should be addressed. Electronic mail: [daniel\\_mennitt@partner.nps.gov](mailto:daniel_mennitt@partner.nps.gov)

variables represent acoustic sources and drive sound pressure levels. Section V focuses on applications of the optimized models to produce visual representations of the acoustical landscape, using the example of a region in southeastern Utah region including Zion National Park. Scenarios were processed to estimate the relative contributions of anthropogenic and natural sounds to ambient sound levels.

A digression is merited to distinguish the approach taken in this paper from the many noise modeling tools that are routinely utilized for transportation and land use planning. In general, these models specify the noise output of a source and predict the attenuation of that energy as it propagates to hypothetical receiver locations.<sup>18</sup> These models incorporate varying amounts of information about the physics of propagation and pertinent environment factors (e.g., terrain, ground cover, and windspeed).<sup>19–21</sup> This approach is convenient when noise can be approximated as originating from a point or a line, as when vehicles or machinery have a high acoustic power relative to their size, and the number of sources is small. An atypical application of this modeling framework is Miller's treatment of sounds from wind blowing through vegetation. *A*-weighted sound levels were predicted given wind speed and observer distance; trees were considered sources with strength increasing with visible surface area.<sup>11</sup> Semi-empirical analytical models have been developed to predict the one-third octave spectra generated by wind in deciduous and coniferous forests.<sup>8–10</sup>

In natural environments, explicit source modeling will usually be impractical because of the indefinite number of sources and their dispersed spatial distribution. Instead, some studies have focused on empirical relationships and parametric models utilizing a diffuse field concept, where over a given area there is a uniformly distributed source and the sound level is assumed to be homogenous. For example, Boersma<sup>7</sup> has shown frequency piecewise linear relationships between the  $L_{95}$  and logarithm of wind velocity in remote, flat, uniformly open agricultural grassland during the summer. Miller<sup>11</sup> formulated a relationship between the rate of rainfall and sound pressure level for an area with consistent ground conditions and vegetation. In general, observations suggest that there are consistent trends in the spectrum of the sound given geospatial features such as topography, vegetation, wind, and water action.<sup>1</sup> These characteristics influence both propagation and the type and intensity of sources present. A recent study<sup>6</sup> documented consistent, distinctive spectral profiles in different forest types attributed to multiple habitat-dependent sound sources. The potential influence of ecological gradients on geophysical, biological, and anthropogenic contributions to the soundscape has been discussed in a special issue of *Landscape Ecology*.<sup>2</sup> The approach presented in this paper is based on the diffuse field concept cited above but allows for contributions from multiple overlapping fields.

## II. DATA

### A. Acoustical data

The sound pressure level data used as the dependent variables in in this study come from the archive of NPS

acoustical measurements collected in National Park units during the years from 2000 to 2011. For this study, seasonal daytime exceedance levels were derived from one second  $L_{eq}$  measurements in 33 one-third octave bands from 12.5–20 000 Hz. For example, the  $L_{90}$  exceedance level is the sound pressure level exceeded 90% of the hour (representing the quietest 10% of the hour). Different exceedance values are influenced by different sources: the  $L_{90}$  will include the consistent roar of river rapids but omit contributions from sparse animal vocalizations.

These measurements were made using ANSI type 1 sound level meters using 1.27 cm measurement microphones deployed 1.5 m above ground, with the microphone enclosed in a cylindrical foam windscreen measuring 10 cm in diameter by 20 cm in length. Audio recordings were also collected to enable identification of sound events. Equipment configurations evolved as battery and electronics technology created opportunities for longer and higher quality recordings with fewer interruptions.<sup>4</sup> Figure 1 depicts a typical site location and the associated equipment.

These data were censored to reduce artifacts of the measurement process. Outdoor recordings, especially in low sound level conditions, are susceptible to spurious levels generated by turbulence around the microphone itself as it obstructs the flow of wind.<sup>7</sup> Although windscreens are designed to mitigate the magnitude of the turbulent wake created, these artifacts are not eliminated. Accordingly, data collected during wind speeds greater than 5 m/s were removed. Data containing other artifacts due to technician interruptions for site maintenance, faulty equipment, etc., were also removed.

In total, 270 316 h from 190 geographically unique sites were incorporated. These sites were distributed across 41 national parks in the contiguous United States, see Fig. 2. Although the sites were located at a wide range of latitudes and longitudes, the Colorado Plateau—especially Grand Canyon National Park—was disproportionately sampled because much of the data were collected to support air tour management.

Ambient sound pressure levels change with time, exhibiting cycles on daily, seasonal, and annual scales. To obtain



FIG. 1. Typical equipment configuration of a long term acoustical monitoring site.

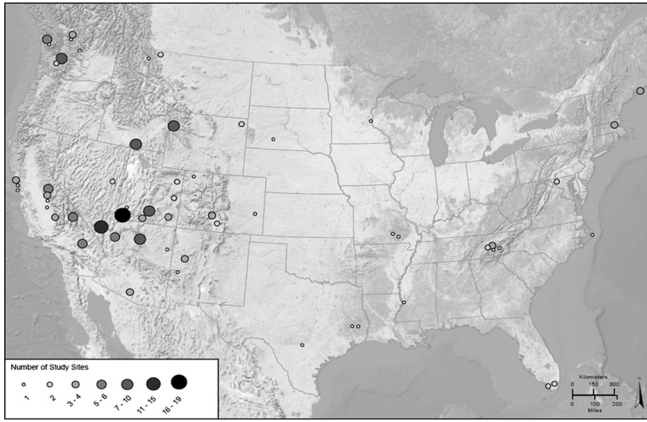


FIG. 2. Locations of the 190 contiguous U.S. site locations.

a consistent estimate of seasonal conditions, studies have shown that a 25 day monitoring period is required to yield a standard error of approximately 3 dB for summary statistics.<sup>22</sup> Twenty-five days from a single season are generally sufficient to capture a representative sample of seasonal weather conditions at a site. All available daytime hours (defined as the hours between 7 a.m. and 7 p.m.) from each deployment were aggregated to yield an estimate of daytime levels. Initially, the sound pressure level (SPL) exceedance values are calculated for each hour. The daytime hour values from a given season are aggregated via the median to yield an estimate for the season. Up to four seasonal measurements per site were available, yielding a total of 291 measurements for the dependent variables.

The 291 daytime  $L_{50}$  spectra are plotted in Fig. 3. A wide range of level and some consistent trends are apparent in these spectra. Although 33 degrees of freedom were available, singular value decomposition revealed that these spectra had less than 10 significant modes. The most prominent was the  $1/f$  trend below 1 kHz, commonly observed in soundscapes and other complex systems in which multiple interacting elements

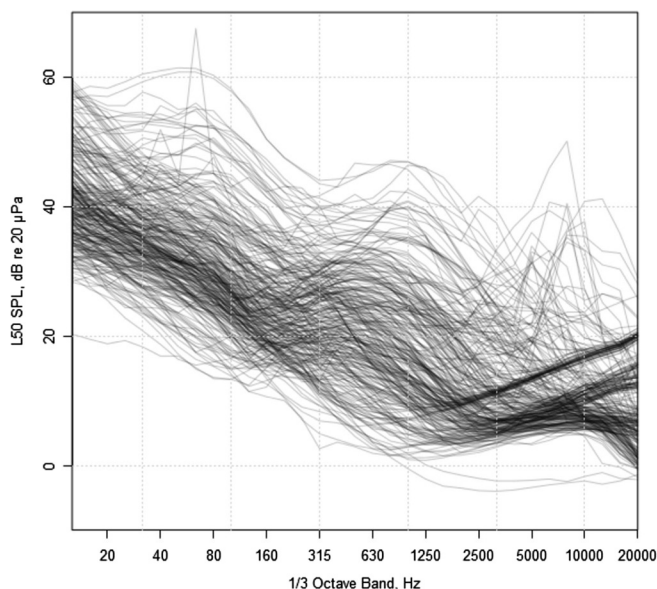


FIG. 3. Seasonal daytime  $L_{50}$  spectrums of all 291 measurements.

coalesce into a group behavior.<sup>3</sup> This stems from the presence of many acoustic sources with low frequency content (e.g., wind, water, and transportation noise) and that the low frequency energy of any source propagates farther than high frequencies due to air absorption, diffraction, ground effects, etc.<sup>23</sup> Other prominent modes represent characteristic site spectra. At frequencies above 1 kHz, limitations in the measurement microphones can be seen: the dark groupings are descriptive of the noise floor of each of the equipment configurations used. The spectra containing one-third octave band values below 0 dB were acquired with low-noise systems in consistently very quiet environments. The data were not corrected for the effects of the instrument noise floor. Noise floor corrections, which degrade the integrity of type 1 sound level meter measurements, are not needed in the range of frequencies most affected by anthropogenic noise.

## B. Explanatory variables

The explanatory variables include geospatial data layers and measurement metadata. For each of the 190 study site locations, potential explanatory variables for sound pressure level were identified and derived based on the literature, authors' previous experience, and data availability (Table I). These explanatory variables have been organized into seven groups: location, climatic, landcover, hydrological, anthropogenic, temporal, and equipment. The majority of explanatory variables originate from geospatial data layers that are readily available across the contiguous United States. The remaining variables, such as time of year and equipment configuration, were recorded during each deployment. Detailed information regarding preparation of explanatory geospatial variables has been published elsewhere.<sup>24</sup>

Location variables included latitude and longitude, elevation derived from a 10 m resolution digital elevation model, slope, and topographic position index (TPI). TPI classifies proximate landform into six categories: flat, ridge, upper slope, middle slope, lower slope, and valleys.

Climatic variables included local precipitation, temperature, and wind power data. Maximum, minimum, and mean temperature and precipitation variables at yearly, summer (June, July, August) and winter (December, January, February) time steps were derived using parameter-elevation regressions on independent slope model climatic data 30-yr average metrics at a 4 km spatial resolution. Wind power categorical potential densities at a height of 50 m ( $W/m^2$ ) were obtained from the Natural Resource Energy Laboratory state level high resolution wind products.

Land cover variables were derived from Anderson level I 2006 National Land Cover Data at 30 m spatial resolution. Level II cover types for forest were also used, to address the sounds produced by wind flowing through trees.<sup>8,9</sup> Land cover variables were represented as the proportion of landcover type within an area of analysis (AOA) surrounding the measurement site (Table I).<sup>25</sup> Multiple AOAs were evaluated for variables in the landcover and anthropogenic categories. Noise from road traffic can travel many kilometers, so at least one AOA had to span this distance. Biological sound sources are more complicated. It is possible to estimate the

TABLE I. Initial potential explanatory variables spatial resolution and description by regression group. Area of interest distances indicate radius of circular area or cylindrical volume centered at site that was considered.

Variable	Area of analysis	Description	Units
Location			
Latitude	Point	Latitude	deg.
Longitude	Point	Longitude	deg.
Elevation	Point	Digital elevation, height above sea level	m
TPI	Point	Topographic position index (e.g., ridge, slope, valley)	categorical
Slope	Point	Rate of change of elevation	deg.
Climatic			
PPTSummer	Point	30 year average summer precipitation	mm
PPTWinter	Point	30 year average winter precipitation	mm
PPTNorms	Point	30 year average yearly precipitation	mm
TMaxSumm	Point	30 year average summer maximum temperature	°C
TMaxWinter	Point	30 year average winter maximum temperature	°C
TMaxNorms	Point	30 year average yearly maximum temperature	°C
TMinSumm	Point	30 year average summer minimum temperature	°C
TMinWinter	Point	30 year average winter maximum temperature	°C
TMinNorms	Point	30 year average yearly minimum temperature	°C
Wind	Point	Wind power class potential density at 50 m	W/m <sup>2</sup>
Landcover			
Dev	200 m, 5 km	Proportion of developed landcover	%
Barren	200 m, 5 km	Proportion of barren landcover	%
Forest	200 m, 5 km	Proportion of forest landcover	%
Deciduous	200 m, 5 km	Proportion of deciduous forest landcover	%
Evergreen	200 m, 5 km	Proportion of evergreen forest landcover	%
Mixed	200 m, 5 km	Proportion of mixed forest landcover	%
Shrub	200 m, 5 km	Proportion of shrubland landcover	%
Herbaceous	200 m, 5 km	Proportion of herbaceous landcover	%
Cultivated	200 m, 5 km	Proportion of cultivated landcover	%
Wetland	200 m, 5 km	Proportion of wetlands landcover	%
Water	200 m, 5 km	Proportion of water (only) landcover	%
Snow	200 m	Proportion of snow landcover	%
Hydrology			
SSlope	16 km	Mean, range and standard deviation of stream slopes	ratio
SSlopeWeight	16 km	Mean, range, and standard deviation of stream slope weighted by DistStreams	ratio/m <sup>2</sup>
DistanceCoast	Point	Distance to nearest coastline	m
DistWaterBody	Point	Distance to nearest body of water	m
DistStreams	Point	Distance to nearest stream	m
DistStreamC	Point	Distance to nearest stream with a Strahler order greater than 1, 3, or 4	m
Anthropogenic			
RddAll	200 m, 5 km	Road density, sum of road lengths (all roads) divided by area of interest	km/km <sup>2</sup>
RddMajor	200 m, 5 km	Road density, sum of road lengths (major roads only) divided by area of interest	km/km <sup>2</sup>
RddWeighted	200 m, 5 km	Road density, sum of road lengths (weighted by class) divided by area of interest	km/km <sup>2</sup>
DistRoadsAll	Point	Distance to nearest road (all roads)	m
DistRoadsMaj	Point	Distance to nearest road (major roads)	m
Naturalness	Point, 5 km	Minimum, maximum, mean, range and standard deviation of naturalness	Naturalness
DistMilitary	Point	Distance to nearest military flight path	m
MilitarySum	40 km	Sum of designated military flight paths	count
FlightFreq	25 km	Total weekly flight observations	count
Wilderness	16 km	Sum of designated wilderness in area of interest	m <sup>2</sup>
Temporal			
dayLength	Point	Average length of day during deployment	hours
circDayY	Point	Annual position, winter/summer	radians
circDayX	Point	Annual position, spring/fall	radians
Equipment			
nf	Point	Noise floor of measurement equipment	dB SPL

range at which the song from a particular bird may be detected given its strength and the background level, but the AOA must be large enough to account for the animal's

capacity to range outside its nominal core habitat. For the results presented here, circular areas of interest with radii of 200 m and 5 km were chosen for the land cover data.

Landcover data provided the first indications that geospatial modeling was likely to be successful. Figure 4 displays the smoothed probability densities of the  $A$ -weighted  $L_{50}$  measurements by majority landcover. Most sites are represented by multiple landcover types, but this plot simply assigns each site to the most common local landcover category. The landcover categories are quite broad; however, snow and cultivated types are not included in Fig. 4 due to especially small sample sizes.

The overall trend in the data is an increasing of sound pressure levels with increasing moisture. Water contributes to the acoustic energy of a soundscape in many ways, most directly through the flow noise of moving water and wave action in larger bodies of water. Water generally promotes vegetative and animal diversity, which introduces new sources of sounds. Last, human settlement is generally associated with water, and human noise is the greatest source of variability in sound levels. This simple example illustrates the potential for geospatial modeling of sound levels, and the substantial variation of sound levels within these landcover classes affirms the need for a multivariate model to incorporate other influential factors and their potential interactions.

Distance to coastline and water bodies were derived from National Hydrography Dataset and NPS Hydrographic Impairment Data. Distances to stream segments by Strahler Calculator stream orders greater than 1, 3, and 4 were derived in GIS using Euclidean distance functions and NHD Plus datasets.<sup>25</sup> GIS was used to derive stream slope mean, range and standard deviation values at a 16 km AOA using NHD Plus stream segments and slope measurements.

Anthropogenic, or human caused, sound is ubiquitous and anthropogenic sources are relatively loud compared to natural sources. This includes transportation noise from aircraft, roadways, railways, snow machines, and water craft, and noise from energy development, resource extraction, cultivation, and communities. The measurements in this study were influenced by anthropogenic noise generated inside and outside park unit boundaries. In addition to the

developed landcover layer, additional geospatial variables were extracted to improve the model's capacity to predict anthropogenic noise. Distances to all roads and major roads were obtained from NPScape roads measure data which is based on source roads data compiled from ESRI39.<sup>25</sup> The sum of road density (1 km spatial resolution) values for all, major, and weighted roads were derived in GIS at several AOA, see Table I. Distance to military flight paths and the sum of designated military flight paths within a 40 km AOA were derived in GIS from department of defense flight path data. Using flight frequency observation data (7 km spatial resolution) sums of weekly flight observations were derived at 25 km AOA. A naturalness index<sup>26</sup> based upon land use, housing density, and road and highway traffic was summarized (maximum, mean, minimum, range, standard deviation, and sum) at 1 and 5 km AOA. Last, the total designated wilderness area was derived at a 16 km AOA.

Much anthropogenic noise, especially energy development and motorized recreation, is not directly captured by the available data layers. For example, visitors contribute to a wide variety of sounds, including hikers walking and talking, motorized recreation and air tours. However, some of this may be captured indirectly. Visitation is correlated with population and developed landcover. Increased visitor activity is also more likely near roads, in moderate climates, and during the summer.

The measurements span the entire year and three temporal variables were included. The dayLength variable represents the average amount of daylight during a measurement; it was derived from the latitude of the site and the time of year of the measurement. The day of year for the measurements has been represented as circular variables, preserving the continuity between December 31 and January 1, by including  $\text{circDayX} = \sin(2\pi \times \text{day}/365)$  and  $\text{circDayY} = \cos(2\pi \times \text{day}/365)$  as covariates.

Finally, some crucial information comes directly from the equipment configuration used to make a given measurement. The combined system noise floor was the lowest expected level for any particular measurement. The equivalent sound pressure level of the noise floor was derived from one-third octave bands measurements and manufacturer's specifications.

### III. METHODS

#### A. Random forests

Most regression models estimate a conditional expectation,  $E(y|X)$ , where  $y$  represents the response or dependent variable (sound level measurements) and  $X$  represents the explanatory or independent variables (geospatial quantities and measurement metadata). This analysis presented several challenges. Many potential explanatory variables were speculative, and multiple variants of some variables were introduced with the intent of identifying the variants with highest predictive power. Nonlinearities and interactions among variables were anticipated. Given uncertainties about the structural form of the best model, and the likelihood that some explanatory variables were irrelevant or redundant, machine learning methods were explored that imposed very few assumptions. Note that these machine learning methods do

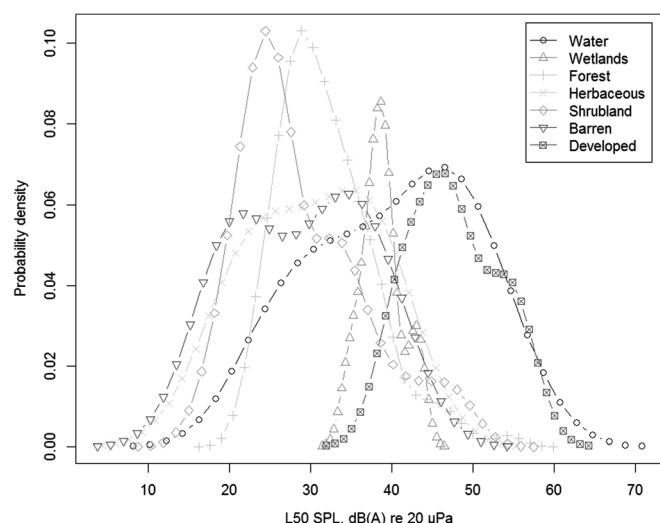


FIG. 4. Probability densities of the  $A$ -weighted  $L_{50}$  measurements categorized by majority landcover. A Gaussian kernel was used to compute the smoothed density estimates.

not fit model parameters in the framework of an assumed structural relationship between the dependent and independent variables.

Under the umbrella of machine learning, many techniques exist with varying degrees of nominal predictive power, interpretability, tunable parameters, robustness, and capacity to deal with mixed data types and potentially irrelevant inputs. In this study, exploratory analyses were investigated with linear models, generalized additive models, support vector machines, and tree-based methods including random forest and boosted regression trees.<sup>27</sup> Preliminary results suggested that tree-based methods had more promise than other methods. Part of this promise was the absence of requirements regarding *a priori* information concerning the form of relationship and interaction among variables.

A random forest is an ensemble of many individual decision trees, as shown in Fig. 5. A decision tree is a statistical model that relates the response  $y$  to explanatory variables  $X$  by recursive binary partitioning of the input data  $X$ . At each node, the data is partitioned into two self-similar subsets, or branches, using simple rules (e.g., elevation greater or less than 1000 m). Binary partitioning is repeated for each new subset until some stopping criterion is reached, such as homogeneity. The classification and regression tree algorithm (CART) creates these partitions by choosing the predictor and criterion to maximize the aggregate response purity in the resulting subsets.<sup>28</sup> The final tree model has  $J$  terminal nodes, or leaves, corresponding to the disjoint regions  $R_j$  that collectively cover the space of all values of the explanatory variables  $X$ . The response  $f(X)$  is predicted with a constant  $b_j$  for  $X \in R_j$ . This is represented by the following additive form:

$$f(X) = \sum_{j=1}^J b_j I\{X \in R_j\}, \quad (1)$$

where the indicator function  $I\{\cdot\}$  has the value 1 if its argument is true and zero otherwise. Because any instance of  $X$  will fall in a single region,  $f(X)$  is essentially predicted by a single constant  $b_j$ . The constant  $b_j$  is obtained by averaging over all the response values of the training data in the leaf,  $R_j$ . Decision trees do not possess coefficients like those found in the general linear model.

The simple decision rules allow for a wide range of relationships to be captured and the hierarchical structure of the tree provides some capacity to account for interactions among the independent variables. However, the locally optimal choice of variables and split criteria may not lead to a globally optimal tree, and decision trees can capture idiosyncratic distinctions in the training data that will not generalize to new data from the same system. Methods such as pruning, boosting and bagging are used to mitigate these problems. Bootstrap aggregating, or bagging, is a type of ensemble learning in which  $T$  decision trees are generated, each with a different bootstrapped sample of the training data.<sup>29</sup> The final prediction,  $\hat{y}$ , is the average over all the individual tree predictions, i.e., aggregating. This mitigates the instability of individual trees and can reduce both bias and variance. By including the fits from an entire ensemble, it is also possible to produce a very flexible model that is able to respond to highly specific, yet systematic features in the data. Finally, by generating a new bootstrapped sample to train each tree a subset of samples that is not used is also created, called out-of-bag (OOB). These samples can be useful for calculating measures of prediction accuracy and variable importance.

One of the most severe drawbacks to ensemble techniques such as bagging is that the direct relationship between input and output of an individual tree is lost in the process. A method for revealing the relationships between explanatory variables and the response variable is addressed in Sec. IV. A random forest is an ensemble of bagged decision trees that has been further randomized by splitting a subset of  $m$  randomly drawn predictor variables at each node.<sup>17</sup> This exploits the benefits of ensemble learning by decreasing correlation between individual tree predictions, i.e., each tree is more independent of the others in the forest. In addition, random forests are able to handle a very large number of explanatory variables, including more independent variables than dependent variable observations. This study utilized the RANDOM FOREST algorithm as it was implemented in R.<sup>30</sup>

## B. Model construction and evaluation

The model construction process included three stages: assessment of independent variable importance, identification of optimal variable sets, and model parameter tuning.

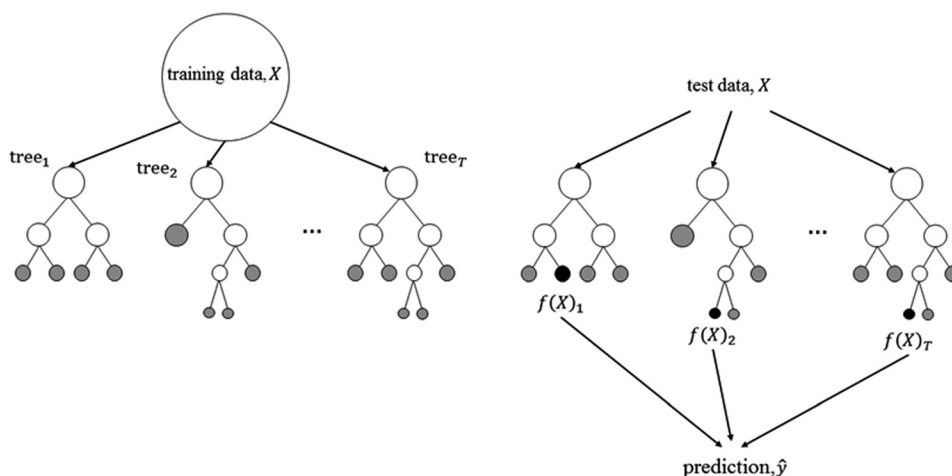


FIG. 5. Conceptual diagram of the RANDOM FOREST algorithm. On the left, trees are trained independently by recursive binary partitioning of a bootstrapped sample of the input data,  $X$ . On the right, test data is dropped down through each tree and the response estimate is the average over all the individual predictions in the forest.

This sequence was used to identify variables that were eliminated without significant degradation in the model's ability to predict sound levels at a new location. Random forests are relatively insensitive to superfluous variables, but unnecessary variables can reduce predictive power. Furthermore, GIS calculation of excess variables is burdensome, and extra variables will complicate interpretation of model results. A simple exhaustive evaluation of all explanatory variable combinations proved computationally infeasible, so a multi-stage process was used.

A separate model was built for each response variable of interest [e.g.,  $L_{90}$  dB(A),  $L_{50}$  500 Hz one-third octave band] for a total of 105 models. The methods outlined in this section were applied to all models. Developing separate models for each response variable identified suites of explanatory variables that provided the best predictions of exceedance statistics for each one-third octave band. Model performance and variable importance measures were challenging to develop for these data. The RANDOM FOREST algorithm calculates an estimate of the mean squared error for each tree using the OOB samples, but this can be misleading.

While RANDOM FOREST error estimates were informative, it was necessary to utilize explicit segmentation of our data to avoid optimistic results. For example, we constructed a random forest model that predicted one-third octave band sound levels, and incorporated frequency as an explanatory parameter. This model revealed that missing one-third octave band measurements could be predicted very accurately from other measurements taken at the same site and time. However, achieving this predictive accuracy required some measurements from every site, so it could not be applied to map sound levels across areas where no measurements had been made.

These correlations extended across time at each site. For example, a site's summer sound pressure level is easier to predict if the winter level is known. Including multiple measurements of a given location in the training data dramatically increases predictive performance. These data are useful for studying how levels change with time or predicting a specific exceedance level at a given location. However, these correlations do not support a spatial model as they overstate the predictability of new locations outside of the training set. A training set that explicitly excluded multiple seasonal measurements from individual sites was needed to identify the predictive value of geospatial variables and provide an unbiased measure of the accuracy of sound level predictions for unmeasured locations. The accuracy of geospatial model performance was assessed by leaving each location out of a model development process, and comparing the predicted and measured values for the omitted location. Unique aspects of the cross validation process are detailed in the following subsections.

### 1. Variable order of importance

The first step in assessing the contributions of variables was to remove highly correlated variables. The linear dependence between all variable pairs was evaluated via the Pearson correlation coefficient. For pairs with correlation greater than 0.95, the variable with the largest absolute mean correlation relative to the entire set was removed.

One method of estimating the relative importance of explanatory variables is to permute the values of a predictor and calculate the change in model performance. This is conveniently implemented within the RANDOM FOREST algorithm as the bagging process generates a test set for each tree. Each variable is permuted in turn while the remaining variables are held constant. The change in error compared to the original OOB error is indicative of the permuted variable's importance. Because the permutation destroys association with other explanatory variables, the importance of multivariate interactions is also taken into account. However, this is a relative measure; no formal inference such as a  $p$ -value is available. Also, determination of the significance of weakly important variables is difficult, as correlations among predictor variables will also influence the variable importance.<sup>31</sup> Therefore, the importance measure was calculated in conjunction with the following process.

Variable importance was determined by an extensive random forest model averaging process. First, the data were divided into four subsets to ensure that no site was represented by more than one seasonal measurement in any of the sets. Random forest models were repeatedly fitted to each of the four data subsets using the default algorithm parameters. Each model iteration within a data subset generated unique variable importance scores, because there are stochastic components in the RANDOM FOREST algorithm. The resultant variable importance measures were averaged across all four data subsets, and averaged across the iterations within each subset. This fitting process was iterated until the mean of the importance measures stabilized. The variable with the lowest importance was removed from the set and the process repeated with the remaining variables. Estimating the weakest variable can be done with more confidence than estimating the entire order concurrently and sequentially dropping variables removes any confounding effects due to correlation with weaker input variables while retaining interactions among useful variables. This stepwise elimination process was not guaranteed to yield the most effective subsets, but it was computationally tractable. Tables III(a)–III(c) show the seven most important variables for the  $L_{10}$ ,  $L_{50}$ , and  $L_{90}$  models, respectively. Interpretation of the covariate rankings in regard to the structure of acoustic environments is discussed in Sec. IV.

### 2. Optimal variable sets

Having ordered the explanatory variables by average importance scores, the next task was to determine how many variables were needed to obtain the most accurate prediction of sound levels at a new site. Thresholds have been proposed to determine the best explanatory variable set using the variable importance measures provided by the RANDOM FOREST algorithm, but these approaches are susceptible to bias and may be misleading.<sup>31</sup> Instead, the variable set that minimized the root-mean-square (rms) error of a leave-one-out (LOO) cross-validation (CV) process was defined as optimal. The LOO CV was implemented by training a random forest model that omitted a measurement, and then comparing the prediction from that model to the omitted measurement. In

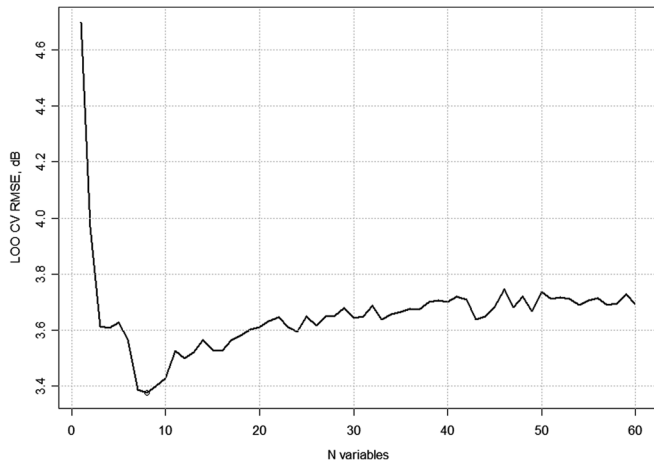


FIG. 6. Determining the optimal variable set for the  $L_{50}$  8 kHz model. The minimum at  $N = 8$  identifies useful variables to be included in the optimal model.

contrast to the subsets used during the variable order of importance step, the training data contained all available measurements during this step. Therefore, measurements from other seasons or years at the location of the omitted measurement were also removed from the training set to avoid misleadingly optimistic results from temporal correlation across observations. This procedure was repeated exhaustively and then averaged over every available measurement, such that the rms error of a variable set was defined as

$$e_{\text{rms}} = \sqrt{\frac{1}{N} \sum_{i=1}^N (y_i - \hat{y}_i)^2}, \quad (2)$$

where  $i$  represented a measurement site and  $N$  was the number of sites. The measurement and prediction has units of dB SPL.

An example of the variable optimization process is shown in Fig. 6 for the  $L_{50}$  model of the 8 kHz band. The prediction accuracy of the model decreases as variables are removed from the training data. These variables, while

assessed a finite importance during the ordering step, are superfluous. The global minimum—the most parsimonious model—occurs at eight variables. Error increases rapidly with fewer than eight variables. The number of important variables as identified by this criterion ranged from 1 to 59 depending on the frequency and exceedance value of interest. The amount of variables is indicative of the both the complexity of the response and the quality of the information available to describe it. For models in which many variables were deemed significant, the majority of predictive power was still carried by the first few variables.

One complication for this process was the role of seasonal variables. The LOO CV process included sites that had measurements from two or more parts of the year. The role of these variables was explicitly omitted from the variable importance assessment, but there are good reasons to anticipate seasonal changes in sound levels. The seasonal variables were reintroduced to the optimal variable set and retained if LOO CV rms error decreased.

### 3. Model parameter tuning

As a final step, the optimal variable set was used to tune the parameters of the random forest model. Several parameters govern the structure of a random forest model.<sup>30</sup> Exhaustive combinations of five parameters were surveyed again using the criterion of LOO CV error: the number of trees in the forest (*ntree*), the sample size presented to each tree (*sampsiz*), the number of variables to evaluate at each split (*mtry*), the minimum node size (*nodesize*), and sampling with or without replacement (*replace*). The best parameter value varied with the response of interest and was related to the number of variables in the optimal model. Overall, minor gains in performance (1% on average) over the default parameters were realized.

### 4. Model performance

The performance of the optimal models after tuning is shown in Fig. 7 by one-third octave bands for the  $L_{90}$

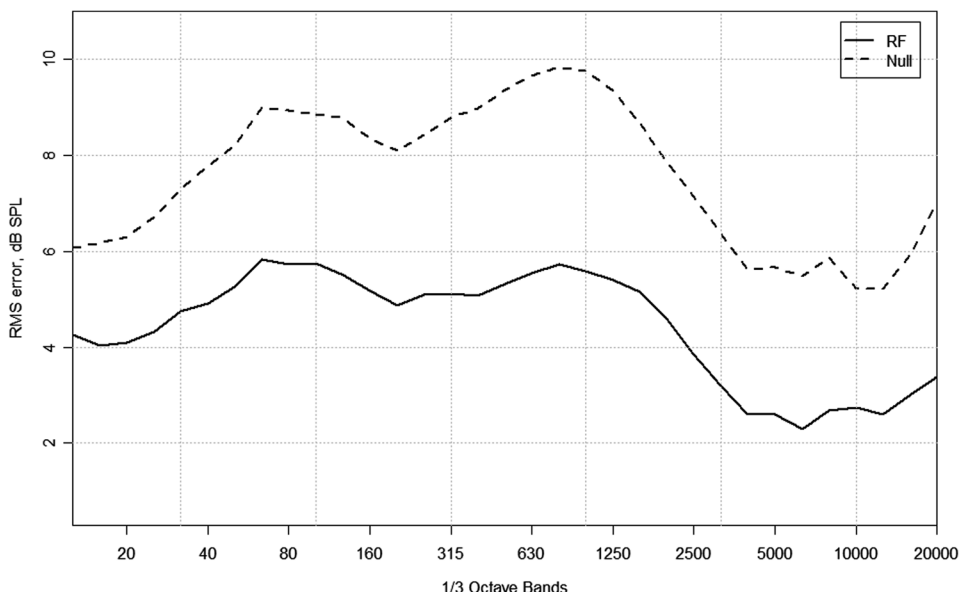


FIG. 7. Performance of the optimal one-third octave band random forest models (rms of the LOO CV error) for the  $L_{90}$  exceedance level. Performance of null models are also shown for reference.

TABLE II. Performance of the optimal random forest (RF) and null models for the wideband response metrics in terms of rms error, median absolute deviation (MAD), and percent variation explained.

	RF rms	Null rms	RF MAD	Null MAD	% explained
$L_{10}$ , dB(A)	4.8	7.3	2.8	4.9	58
$L_{10}$ , dB	5.5	7.6	3.9	5.6	49
$L_{50}$ , dB(A)	4.8	8.1	2.8	5.6	65
$L_{50}$ , dB	5	6.9	3.0	4.5	48
$L_{90}$ , dB(A)	4.8	8.3	2.7	5.2	66
$L_{90}$ , dB	4.3	6.8	2.3	3.9	60

exceedance level. The performance of a null model, equal to the mean of all the sound level measurements  $\bar{y}$ , is shown for comparison. The mean approximates a maximum likelihood estimator of location because the sound level measurements, expressed in decibels, roughly approximate a Gaussian distribution. Results for the wideband A-weighted and unweighted response data appear in Table II. Models fitted to wideband measurements perform slightly better than applying the results of the 33 one-third octave band models to predict wideband levels. The median absolute deviation (MAD) is included to provide a measure of scale that is resistant to outliers. The difference between MAD and rms error indicates the influence of outliers on the rms measure.

For the one-third octave band models, the rms error and MAD followed the trends of the variance in the response data. The magnitude of variation explained is defined as

$$R^2 = 1 - \frac{\sum_{i=1}^N (y_i - \hat{y}_i)^2}{\sum_{i=1}^N (y_i - \bar{y})^2}. \quad (3)$$

Figure 8 plots this measure by one-third octave band for the  $L_{10}$ ,  $L_{50}$ , and  $L_{90}$  exceedance levels. The geospatial model explains progressively more variation in sound levels with

increasing frequency, even though there is more variation across sites in the mid-frequency range (Fig. 7). Figures 3 and 8 suggest that there is substantial complexity of low frequency soundscapes that cannot be explained by the geospatial variables available to these models. Given the nature of outdoor propagation attenuation, it is likely that more sources are present with decreasing frequency and these geospatial models may be underestimating the spatial scale of contributions to low frequency sound level measurements.

Figure 9 shows examples of measured spectra and model predictions. The model fit for individual sites can be quite close, capturing idiosyncratic trends in sound level spectra as shown in Figs. 9(A) and Fig. 9(B). Model errors include abnormal characteristics not well represented by the explanatory variables [Fig. 9(C)] or reasonable agreement in spectral shape with an offset in level [Fig. 9(D)].

These models have been constructed to predict aggregate seasonal metrics of ambient sound pressure levels. The geospatial input data available was of long term averages or relatively constant features. The expected error of estimating the seasonal value using the response data is  $\pm 3$  dB for the 25 days samples in the NPS archive. This sets the lower bound for geospatial model error. The model error is remarkably close to this bound. The close agreement between model and measurement is partly due to the simplifying, summary characteristics of exceedance level metrics. For example, the  $L_{10}$  is largely determined by transient events and is less sensitive to background sound levels, while the  $L_{90}$  represents background levels and is relatively unaffected by transients.

One systematic trend emerged from the residual errors in the geospatial model. Error increased as the prediction diverged from the mean predicted value: loud sites were underestimated and quiet sites were overestimated. Two factors explain this trend. First, extreme sites are often due to factors that are not captured by the geospatial data set. For example, the spectrum in Fig. 9(C) is a site in Zion National Park near Zion Lodge. While the geospatial variables captured the site's proximity to a road, the traffic on this road is unusual: shuttle buses and a small number of administrative

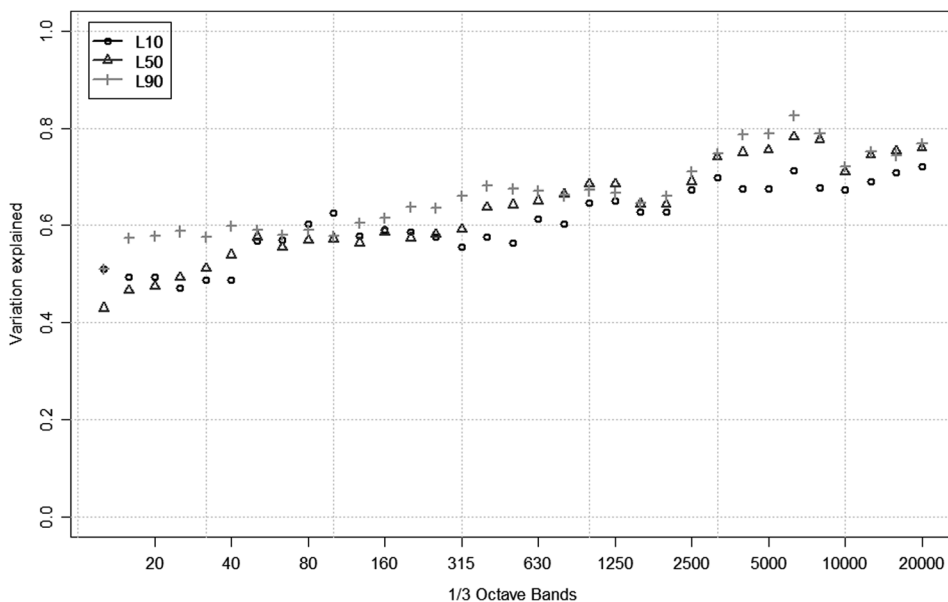


FIG. 8. The variation explained by the optimal random forest models for each one-third octave band and exceedance level.

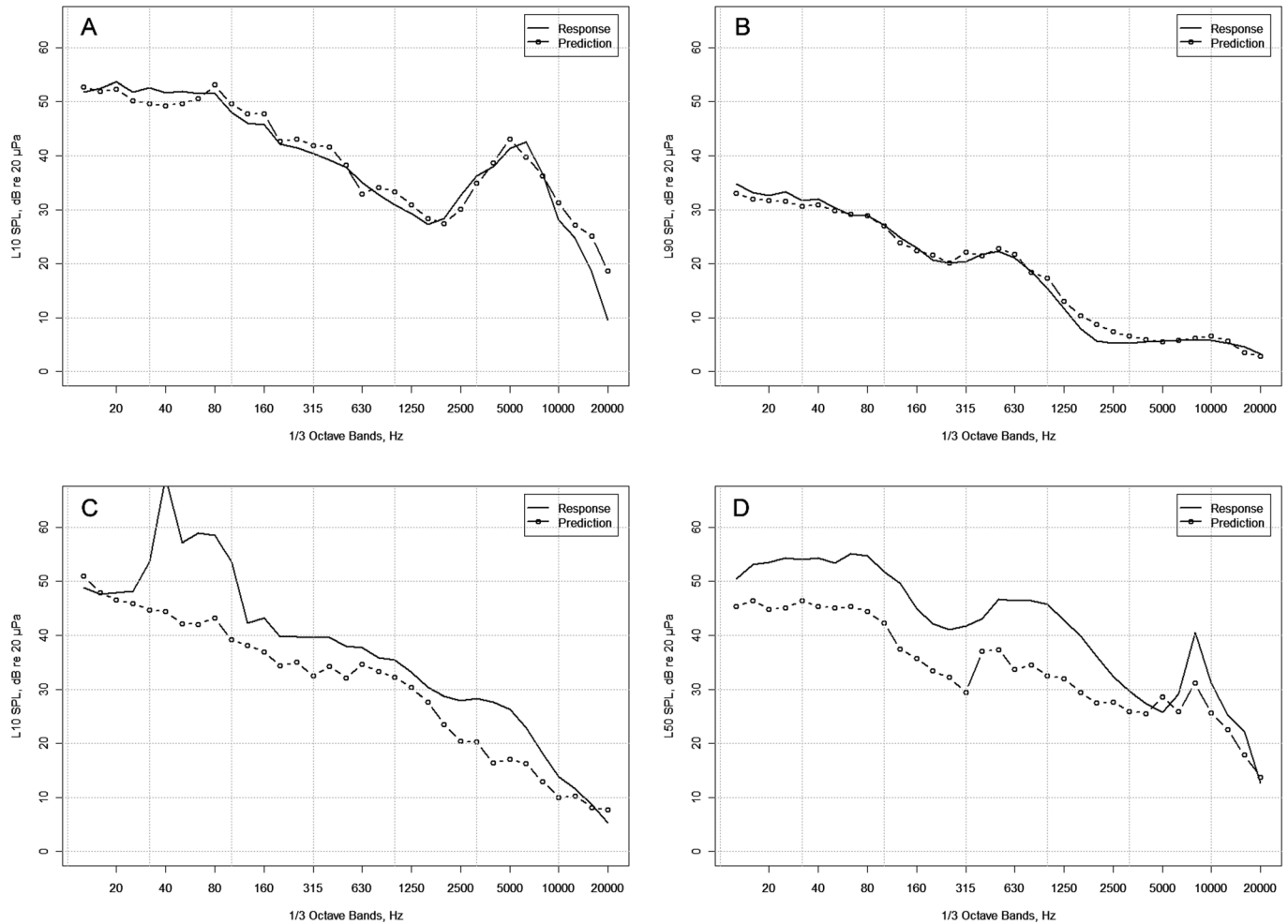


FIG. 9. Example comparisons of the response and model prediction spectra: a riparian area at Monocacy National Battlefield (A), a canyon rim at Grand Canyon National Park (B), a road corridor in Zion National Park (C), and a developed frontcountry area at Vicksburg National Military Park (D).

vehicles. Furthermore, because the site was near a bus stop, higher engine power levels were occurring as the buses accelerated up to cruising speed. Other examples of exceptional conditions that were not captured by geospatial variables were construction projects and road closures.

Two characteristics of the RANDOM FOREST algorithm also contribute to this “regression towards the mean.” The partitions created within individual trees will necessarily lump extreme sites with less extreme sites in the terminal nodes  $R_j$ , introducing one bias towards the mean. Second, the averaging process used to aggregate the predictions of individual trees dilutes the influence of the extreme tree predictions with many other tree predictions that are less extreme. Even if some individual trees have terminal nodes corresponding to extreme SPL, the average vote pulls away from these extremes.

#### IV. THE STRUCTURE OF THE SOUNDSCAPE

##### A. Important geospatial variables

All variable categories (Table I) influence the soundscape in particular areas of the spectrum and time scale. The prevalence of anthropogenic variables is evident by Table III. Anthropogenic is the most common variable category, accounting for about a third of the most powerful

explanatory variables across the spectrum, especially at low frequencies. The sources inherent to developed areas, roads, and aircraft flyovers such as rotating machinery have spectral profiles dominated by low frequency energy. The  $L_{90}$ , which represents persistent sources, has a strong presence of long range anthropogenic variables at low frequencies such as NatMax5km (the maximum naturalness over a 5 km radius area). The  $L_{10}$ , which represents very loud events and short time scales, includes anthropogenic descriptors at higher frequencies and closer ranges (e.g., Dev200m). Although all of the sites are within national parks, acoustical environments transcend park boundaries.

Climatic variables are the second most prevalent category, and precipitation is the most important driver for long term levels in the 200 to 1250 Hz range. In addition to the sound directly generated by active precipitation, it has been observed that wind-induced energy often dominates these frequencies; the impact of wind on sound pressure levels is largely dependent on the present vegetation or lack thereof.<sup>1,6–11</sup> Rustling leaves and other mechanical agitation of plants generates sound in this frequency range, and the quantity and variety of vegetation increases with precipitation. It is likely that precipitation indirectly predicts the volume and diversity of biological choruses, as mesic habitats often promote a greater diversity and concentration of plant

TABLE III(a). A subset of the explanatory variables for the 33 one-third octave band  $L_{10}$  models ranked by relative importance. The most important variable is in column 1 and subsequent variables proceed in decreasing order to the right.

Frequency (Hz)	1	2	3	4	5	6	7
12.5	PPTNorms	Forest200m	Latitude	SSlopeStd	TMaxWinter	Forest5km	SSlopeMean
15.8	PPTNorms	TMinWinter	Latitude	TMaxWinter	Forest200m	SSlopeStd	SSlopeMean
20	Latitude	TMinWinter	TMaxWinter	PPTNorms	Forest5km	TMinSumm	Flights25km
25	TMinWinter	Latitude	TMaxWinter	Flights25km	TMinSumm	PPTNorms	nf4
31.5	Flights25km	TMinSumm	Latitude	TMinWinter	TMaxWinter	Dev200m	PPTNorms
40	Flights25km	Latitude	Dev200m	TMinSumm	TMinWinter	TMaxWinter	DistRoadsMaj
50	TMinSumm	Dev200m	Flights25km	Latitude	TMinWinter	TMaxWinter	NatMax5km
63	Dev200m	TMinSumm	NatMax5km	NatPoint	TMinWinter	TMaxWinter	Flights25km
80	Dev200m	TMinSumm	NatPoint	TMaxSumm	NatMax5km	Flights25km	DistRoadsMaj
100	Dev200m	Flights25km	TMinSumm	RddMajor5km	TMaxSumm	DistRoadsMaj	TMinWinter
125	Flights25km	Dev200m	Latitude	RddMajor5km	TMinSumm	TMinWinter	TMaxSumm
160	Flights25km	Dev200m	Latitude	NatMax5km	TMaxWinter	NatPoint	TMaxSumm
200	Flights25km	Dev200m	TMaxWinter	NatMax5km	NatPoint	TMinWinter	Latitude
250	Flights25km	Dev200m	NatMax5km	TMaxWinter	NatPoint	TMinWinter	Dev5km
315	Dev200m	Flights25km	NatMax5km	NatPoint	DistStreamC3	Latitude	Dev5km
400	Dev200m	Flights25km	Shrub200m	DistStreamC3	Shrub5km	Dev5km	RddMajor5km
500	Dev200m	Shrub200m	Flights25km	DistStreamC3	Shrub5km	Dev5km	RddMajor5km
630	Dev200m	Shrub200m	Shrub5km	DistStreamC3	Elevation	NatMax5km	Dev5km
800	Dev200m	Shrub200m	Shrub5km	DistStreamC3	Elevation	NatMax5km	Forest5km
1000	Dev200m	Shrub200m	Shrub5km	DistStreamC3	Elevation	Forest5km	SSlopeMean
1250	Dev200m	Shrub200m	Shrub5km	DistStreamC3	Elevation	DistRoadsMaj	Forest200m
1600	Dev200m	Shrub200m	Shrub5km	DistStreamC3	Elevation	DistRoadsMaj	Forest200m
2000	Dev200m	nf23	Shrub200m	Shrub5km	Forest200m	Elevation	PPTNorms
2500	Dev200m	nf24	Shrub5km	PPTNorms	Evergreen5km	Elevation	Shrub200m
3150	nf25	PPTNorms	Longitude	Dev200m	dayLength	Shrub5km	Evergreen5km
4000	nf26	Elevation	dayLength	PPTNorms	Longitude	DistStreamC3	Shrub5km
5000	nf27	Longitude	dayLength	Elevation	DistStreamC3	PPTNorms	Shrub5km
6300	nf28	Longitude	Elevation	Deciduous5km	dayLength	DistStreamC3	Wetland200m
8000	nf29	Longitude	Elevation	Deciduous5km	SSlopeMean	Wetland200m	DistStreamC3
10 000	nf30	Longitude	Elevation	DistStreamC1	Wetland200m	Dev5km	RddMajor5km
12 500	nf31	DistStreamC1	Dev5km	RddMajor5km	Wetland200m	Elevation	Longitude
16 000	nf32	NatRange5km	NatMIN5km	NatSTD5km	Dev5km	DistStreamC1	DistStreamC3
20 000	nf33	NatRange5km	NatMIN5km	NatSTD5km	NatMax5km	PPTSummer	TMinSumm

and animal species.<sup>32</sup> The acoustical consequences of higher ecological productivity and species diversity will often include higher biological sound levels across a broad range of frequencies.<sup>33</sup>

Although wind was not identified as a variable with significant predictive power, wind related sound is a pervasive natural phenomenon. Most models of outdoor sound pressure levels have considered some aspect of wind. Wind generates sound by several mechanisms. At low frequencies, high levels can be generated due to the hydrodynamic pressure fluctuations generated by turbulent flow. Sounds are generated by flow over and around obstacles (e.g., buildings, tree trunks, coniferous needles) as well as radiation from mechanical contact between elements excited into motion by wind (e.g., rustling leaves, creaking branches).<sup>7</sup>

Two factors explain the absence of a wind variable from our geospatial models. First, sounds caused by wind are probably responsible for some of the contributions of the landcover, precipitation, temporal, and location variables to sound level prediction. The spectral shape of wind-induced vegetation sound can be independent of wind speed for some plant communities.<sup>8,9</sup> Second, the wind data layer addressed wind speed

at 50 m height above ground. Measured wind data at a height of 1.5 m were available for a subset of the monitoring sites. Exploratory random forest models using measured wind speed at 1.5 m revealed significant contributions to one-third octave bands below 100 Hz, and lesser effects at higher frequencies. If a continental scale wind data layer addressing lower altitude wind speeds or turbulent fluctuation strength were available, it would likely improve the model performance.

In addition to natural sources of wind sounds, turbulent flow around the microphone and windscreen contributes an artifact to all sound level measurements. These artificial contributions were mitigated in this study by using appropriate microphone windscreens and removing acoustic measurements during wind speeds of 5 m/s or greater.

One of the most salient characteristics of Table III is the groupings of some variables in importance ranking across adjacent one-third octave bands. This trend is directly connected to the exploratory singular value decomposition analysis described in Sec. II: although 33 one-third octave bands are available, a lower resolution is sufficient to capture the dominant trends in the seasonal daytime soundscape. For example, the DistStreamC3 (distance to a stream of Strahler

TABLE III(b). A subset of the explanatory variables for the 33 one-third octave band  $L_{50}$  models ranked by relative importance. The most important variable is in column 1 and subsequent variables proceed in decreasing order to the right.

Frequency (Hz)	1	2	3	4	5	6	7
12.5	TMinWinter	SSlopeStd	Longitude	TMaxWinter	Flights25km	Latitude	TMinSumm
15.8	Flights25km	TMaxWinter	Latitude	TMinWinter	SSlopeStd	TMinSumm	Longitude
20	TMinWinter	Flights25km	Latitude	TMaxWinter	SSlopeRange	TMinSumm	NatMax5km
25	TMinWinter	NatMax5km	Flights25km	TMaxWinter	SSlopeRange	Dev200m	TMinSumm
31.5	NatMax5km	TMinWinter	NatPoint	Dev200m	TMinSumm	NatMIN5km	Shrub5km
40	NatMax5km	TMinWinter	Dev200m	NatPoint	TMaxWinter	NatMIN5km	TMinSumm
50	NatMax5km	TMinWinter	Dev200m	NatPoint	TMaxWinter	NatMIN5km	TMinSumm
63	NatMax5km	Dev200m	TMinWinter	NatPoint	TMaxWinter	Dev5km	NatMIN5km
80	NatMax5km	TMaxWinter	NatPoint	Dev200m	TMinWinter	NatMIN5km	Dev5km
100	NatMax5km	TMaxWinter	Dev200m	NatPoint	TMinWinter	Dev5km	NatMIN5km
125	NatMax5km	Dev200m	TMaxWinter	NatPoint	TMinWinter	Dev5km	NatMIN5km
160	NatMax5km	NatPoint	TMinWinter	Dev200m	Flights25km	NatMIN5km	DistRoadsAll
200	NatMax5km	Dev200m	NatPoint	TMinWinter	Shrub5km	Shrub200m	NatMIN5km
250	NatMax5km	Elevation	Shrub200m	Shrub5km	NatPoint	Dev200m	Forest5km
315	DistStreamC3	Shrub200m	Shrub5km	Elevation	NatMax5km	NatPoint	Forest200m
400	Shrub200m	DistStreamC3	Shrub5km	NatMax5km	NatPoint	PPTWinter	Forest200m
500	Shrub200m	DistStreamC3	Shrub5km	NatMax5km	NatPoint	Forest200m	PPTWinter
630	Dev200m	Shrub200m	Shrub5km	DistStreamC3	Forest200m	Elevation	PPTWinter
800	Dev200m	Shrub200m	Shrub5km	DistStreamC3	Forest200m	Elevation	PPTNorms
1000	PPTNorms	Forest200m	DistStreamC3	Elevation	Shrub200m	Dev200m	Shrub5km
1250	PPTNorms	DistStreamC3	Forest200m	Dev200m	Elevation	Shrub200m	Shrub5km
1600	nf22	Shrub5km	Dev200m	DistStreamC3	Forest200m	PPTNorms	Shrub200m
2000	nf23	Shrub5km	Dev200m	DistStreamC3	PPTNorms	Forest200m	Elevation
2500	nf24	Shrub5km	DistStreamC3	Elevation	PPTNorms	Evergreen200m	PPTSummer
3150	nf25	Longitude	DistStreamC3	Shrub5km	PPTSummer	NatMax5km	Evergreen5km
4000	nf26	Longitude	DistStreamC3	PPTSummer	NatMax5km	Shrub5km	Evergreen5km
5000	nf27	Longitude	Elevation	DistStreamC3	PPTSummer	Wetland200m	DistStreamC4
6300	nf28	Longitude	Elevation	Wilderness	Wetland5km	DistStreamC4	PPTSummer
8000	nf29	Elevation	Longitude	PPTSummer	DistStreamC3	Dev5km	DistStreamC1
10 000	nf30	PPTSummer	DistStreamC3	Longitude	DistStreamC1	Dev5km	RddMajor5km
12 500	nf31	DistStreamC3	PPTSummer	DistStreamC1	TMaxWinter	TMinWinter	TMaxSumm
16 000	nf32	DistMilitary	MilitarySum	TMinSumm	TMaxSumm	DistStreamC3	TMinWinter
20 000	nf33	PPTSummer	NatMax5km	TMaxSumm	TMinSumm	Longitude	Shrub5km

categorization class 3 or lower) variable is very important for the 315–1000 Hz one-third octave bands. The importance diminishes for groups of one-third octave bands at progressively high frequencies.

The noise floor of the equipment used was the most powerful predictor of high frequency sound levels due to the quantity of response data at the noise floor. The extent of the spectrum explained by the noise floor increases with exceedance levels, becoming most prominent in the  $L_{90}$  models. Properly accounting for artifacts introduced by varying equipment packages allows for better model performance and interpretation.

The results discussed herein are a consequence of the available sample. Variables identified as not important through this process were not necessarily irrelevant to sound level measurements. They simply did not make sufficient independent contribution to the predictive power of this model. For example, distance to coastline is relevant to sound pressure level over a limited range of distances. Beyond this distance, the acoustic energy from surf is negligible and the variable is essentially noise. More measurements or alternate formulations of the available GIS data may yield variables that make a significant contribution in future models.

## B. Quantifying the influence of variables across a gradient

The RANDOM FOREST algorithm generates predictive models that can encompass a wide range of relationships between the independent and dependent variables. The structure of these models responsible for this flexibility also inhibits the process of diagnosing or interpreting the contributions of each independent variable. One method for addressing this need is to compute partial dependence functions for each of the independent variables.<sup>31,34</sup> Consider a subset of explanatory variables  $\mathbf{z}_s \subset \mathbf{X}$  and the complement subset  $\mathbf{z}_c$ . The partial dependence function is the average response of the model over all of the available training data for permuted values of  $\mathbf{z}_s$ :

$$\bar{y} = \frac{1}{N} \sum_{i=1}^N \hat{y}(\mathbf{z}_s, \mathbf{z}_{c,i}). \quad (4)$$

The influence of the predictor  $\mathbf{z}_s$  across a gradient can be quantified by specifying a sequence of values and calculating  $\bar{y}$  for each. Plots of the partial dependence function show how the average response varies with a given predictor while

TABLE III(c). A subset of the explanatory variables for the 33 one-third octave band  $L_{90}$  models ranked by relative importance. The most important variable is in column 1 and subsequent variables proceed in decreasing order to the right.

Frequency (Hz)	1	2	3	4	5	6	7
12.5	NatMax5km	TMinWinter	NatPoint	Elevation	NatMIN5km	Mixed5km	Shrub5km
15.8	Elevation	NatMax5km	TMinWinter	NatPoint	NatMIN5km	Shrub5km	Dev5km
20	Elevation	NatMax5km	TMinWinter	NatPoint	Shrub5km	Dev5km	RddMajor5km
25	Elevation	NatMax5km	NatPoint	TMinWinter	Dev5km	RddMajor5km	TMaxWinter
31.5	NatMax5km	NatPoint	Elevation	NatMIN5km	TMinWinter	Dev200m	Dev5km
40	NatMax5km	NatPoint	TMinWinter	Dev5km	NatMIN5km	Elevation	DistStreamC3
50	NatMax5km	Elevation	NatPoint	Dev200m	TMinWinter	NatMIN5km	Dev5km
63	Elevation	NatMax5km	Dev5km	NatPoint	Dev200m	NatMIN5km	TMinWinter
80	NatMax5km	Elevation	Dev200m	NatPoint	Dev5km	NatMIN5km	TMinWinter
100	NatMax5km	Elevation	Dev5km	Dev200m	NatPoint	NatMIN5km	RddMajor5km
125	NatMax5km	NatPoint	Elevation	Dev200m	Dev5km	NatMIN5km	Shrub5km
160	NatMax5km	NatPoint	Elevation	NatMIN5km	Shrub5km	Shrub200m	DistStreamC3
200	PPTNorms	Elevation	NatMax5km	Shrub200m	NatPoint	Shrub5km	DistStreamC3
250	PPTNorms	Elevation	Shrub200m	DistStreamC3	NatMax5km	Shrub5km	NatPoint
315	PPTNorms	DistStreamC3	Shrub200m	Elevation	NatMIN5km	PPTWinter	Forest200m
400	PPTNorms	DistStreamC3	Shrub200m	Elevation	PPTWinter	Forest200m	NatMIN5km
500	PPTNorms	DistStreamC3	Forest200m	Elevation	Shrub200m	PPTWinter	NatMIN5km
630	PPTNorms	DistStreamC3	Forest200m	Elevation	PPTWinter	Shrub200m	NatMIN5km
800	PPTNorms	DistStreamC3	Forest200m	Elevation	PPTWinter	Shrub200m	NatMax5km
1000	PPTNorms	DistStreamC3	Forest200m	Elevation	PPTWinter	Shrub200m	Shrub5km
1250	PPTNorms	nf21	DistStreamC3	Forest200m	Elevation	PPTWinter	Shrub200m
1600	nf22	PPTNorms	DistStreamC3	Forest200m	Elevation	PPTWinter	Shrub5km
2000	nf23	Shrub5km	DistStreamC3	PPTNorms	Forest200m	Elevation	PPTSummer
2500	nf24	PPTSummer	DistStreamC3	Shrub5km	PPTNorms	Elevation	Forest200m
3150	nf25	PPTSummer	DistStreamC3	Shrub5km	NatMax5km	Longitude	Mixed5km
4000	nf26	Longitude	PPTSummer	DistStreamC3	Shrub5km	NatMax5km	Elevation
5000	nf27	Longitude	PPTSummer	DistStreamC3	Elevation	Shrub5km	Wetland5km
6300	nf28	Longitude	PPTSummer	DistStreamC3	Wetland5km	Elevation	Wilderness
8000	nf29	PPTSummer	DistStreamC3	Dev5km	Elevation	Longitude	SSlopeStd
10 000	nf30	TMaxSumm	PPTNorms	TMinSumm	PPTWinter	Latitude	Dev5km
12 500	nf31	TMaxSumm	TMinSumm	MilitarySum	Latitude	DistMilitary	TMinWinter
16 000	nf32	MilitarySum	DistMilitary	TMaxSumm	TMinSumm	TMinWinter	Flights25km
20 000	nf33	Longitude	Shrub5km	TMaxSumm	TMinSumm	PPTSummer	NatMax5km

the values of all other predictors,  $z_c$ , are fixed at their base levels. The more the dependence of  $\hat{y}$  on  $z_s$  is purely additive or multiplicative, the more the partial dependence plot provides a complete description of the variable's influence. In any case, a causal relationship is not claimed. Interactions can be analyzed by allowing the subset  $z_s$  to include multiple explanatory variables.

Partial dependence plots for the explanatory variables have been calculated and examples appear in Fig. 10. The dependence functions were calculated independently for each one-third octave band model and then normalized by subtracting the mean response. The functions from each band were concatenated to yield the composite influence of the explanatory variable across the spectrum. Partial dependence plots also suggest the possibility of manipulating variable values to generate scenarios, as discussed further in Sec. V.

### C. Interpreting the contributions of independent variables

Geospatial variables have complex relationships with measured sound levels, incorporating aspects of sound

generation and sound propagation. A single variable can simultaneously influence many different, sometimes conflicting drivers of the sound pressure level. For example, foliage can attenuate propagating sound,<sup>23</sup> wind flowing through vegetation generates sound, and the biological habitats that vegetation creates are home to animal sources of acoustic energy. Diagnosing the aggregate spectral contributions of geospatial variables helps identify the mechanisms involved, and offers some qualitative assurance that the complex modeling effort has yielded a plausible outcome.

Location, a deterministic variable that does not change over time, is possibly the simplest predictor variable. In the limit of sufficiently dense sampling, predictions could be made based solely on interpolation from neighbors.<sup>14,35</sup> While proximity does not play a role in sparsely sampled data sets, ambient sound pressure levels are location dependent. The primary longitudinal trend exhibited by the model is increased levels on the east coast relative to the rest of the country, likely due to increased human development. Latitude, along with elevation, influences the presence and type of vegetation and wildlife habitats. Elevation is also correlated with wind speed and complexity of terrain. A

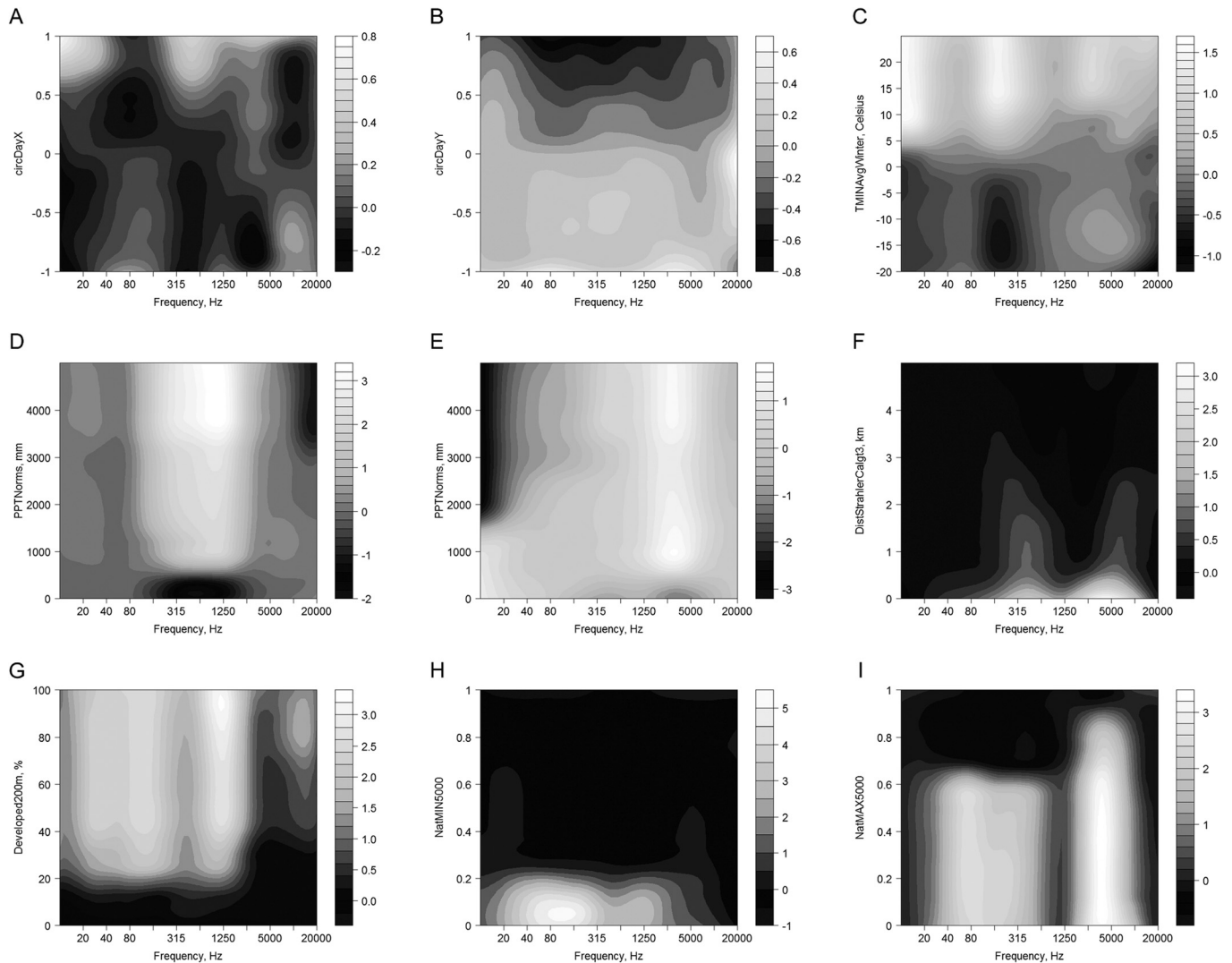


FIG. 10. Partial dependence functions for all 33 one-third octave band models considering a single variable. Intensity represents the change from the mean response, averaged over all samples in the training set. Examples are of the  $L_{10}$  circDayX (A),  $L_{50}$  circDayY (B),  $L_{50}$  TMinWinter (C),  $L_{90}$  PPTNorms (D),  $L_{10}$  PPTNorms (E),  $L_{10}$  DistStreamC3 (F),  $L_{90}$  Dev200m (G),  $L_{90}$  NatMin5km (H), and  $L_{10}$  NatMax5km (I).

ridge top allows for greater wind exposure and unobstructed propagation paths from acoustic sources whereas canyons create sheltered areas that promote development of temperature inversions and have the ability to channel sound through reflection and refraction.

Climatic variables influence sound levels due to propagation and sound source effects. Sound propagation is modulated by vertical sound speed profiles, especially temperature inversions. Nights in the winter are much longer than nights during the summer, so surface inversions are stronger and more common during the winter months. Strong temperature and pressure gradients also create seasonal variation in wind speeds, with maxima in winter and spring and minima in summer and autumn. Biological activity is affected by climate and time, with more abundant vegetation and more bioacoustical activity during warmer times of year. The partial dependence of the  $L_{10}$  on circDayX appears in Fig. 10(A). Increased levels during the fall (circDayX = -1) at very high frequencies is consistent with the pattern of increased insect activity until the first freeze. The partial dependence of the  $L_{50}$  on circDayY appears in Fig. 10(B). Across a wide

range of frequencies, winter levels (circDayY = 1) are quieter on average than summertime levels. This could be attributed to the absorptive properties of snow, the loss of foliage, and lower levels of wildlife and human activity (in park settings). This trend is supported by the magnitude of temperature during a given season. Partial dependence plots of temperature variables, for example the  $L_{50}$  TMinWinter in Fig. 10(C), also share a strong trend of increasing sound pressure level with temperature. Higher temperatures correlated with increased insect abundance and activity. Cicadas are among the loudest insects, producing sounds up to 120 dB SPL, and their influence can be seen in Fig. 9(a) around 5 kHz. Higher temperatures can lead to unstable atmospheric profiles, which combine with moisture to create thunderstorms. The low frequency sounds from these storms can travel hundreds of kilometers and may be responsible for the low frequency increase in Fig. 10(C) and the partial dependence functions of other temperature variables, the behavior of which is similar to TMinWinter.

Landcover can influence both acoustic propagation and the geophysical, biological, and anthropogenic sources present.

Landcover has often been used as the primary designator for acoustic zones.<sup>5</sup> Recent empirical studies have shown habitat-dependent sound level characteristics where the spectrums of sites within a landcover type are more similar than closer proximity sites in an area of different landcover.<sup>6</sup> Another study showed statistically significant similarities between multiple measurements within a habitat and differences across two habitats (treed mountaintop and grassy hilltop).<sup>36</sup>

Most sites in the NPS archive were primarily composed of forest or shrubland landcover types. Forest, shrubland, and developed landcover types had the greatest influence on sound levels. The partial dependence of Forest200m on  $L_{90}$  shows some increased energy in the range of wind induced vegetation noise. The partial dependence is a relatively minor effect. However, forest landcover sites were very common in the sample, so they likely influenced the mean spectrum and thereby reduced the direct influence of this landcover factor. A forest effect may also explain aspects of the partial dependence plot of  $L_{10}$  Shrub5km, as a shrubland and forest cover are inversely related. Very low proportions of shrubland predicted increased energy at 4 kHz, likely due to an increase in forest cover (possibly deciduous trees).

Precipitation is a source of acoustic energy when it is actively raining, hailing or thundering, although in cold climates (winter season, high elevations, and/or high latitudes) the highly absorptive properties of soft snow can have the opposite effect. The level of precipitation perhaps more importantly influences the type of vegetation present and is likely to add energy to the soundscape through wind-induced vegetation noise. This energy is prominent in the 200 Hz to 2 kHz range for conifers and 5 kHz and higher for deciduous trees.<sup>8,9</sup> The precipitation variables have the strongest influence on the  $L_{90}$  metric, which represents background levels and persistent sound sources. As evident from the partial dependence plot of  $L_{90}$  PPTNorms, the amount of precipitation has a strong influence in the mid frequency range [Fig. 10(D)], whereas  $L_{10}$  PPTNorms shows influence at higher frequencies, perhaps due directly to rain, dripping water, or other weather events [Fig. 10(E)]. In general, the  $L_{10}$  has stronger high frequency content than the lower exceedance levels. The loudest events are likely closer to the receiver and therefore not subject to atmospheric absorption and other effects of long-range propagation.

Although the amount of precipitation is proportional to snowpack and subsequently related to the energy of flowing water, that effect is distributed over a wide area often far from the area of analysis. The distance to streams group of predictors was the most influential hydrological variable. The partial dependence plot of the  $L_{10}$  DistStreamC3 is shown in Fig. 10(F) and contribution to both mid and high frequency energy are clearly distinct ( $L_{50}$  similar). The partial dependence function is not necessarily the spectrum of a river, but the spectrum that explains the acoustic conditions near a river considering all other sources and the interactions with other variables. The high frequency energy is most likely a result of increased birdsong in riparian areas and this effect can be seen clearly in the spectrums of Figs. 9(A) and 9(D). The energy from the actual water action is lower in frequency, e.g., the distant Colorado River is responsible for

the energy centered around 600 Hz in Fig. 9(B). Increased levels during the spring in the frequency range centered about 600 Hz is also likely a result of snowmelt [Fig. 10(A)].

The anthropogenic variables have a broad influence across the spectrum. The consequence of increasing anthropogenic activity is always increased sound pressure levels. Generally, variables on shorter spatial scales (point and 200 m) are necessary to explain the energy at higher frequencies in quieter exceedance levels [ $L_{90}$  Dev200m, Fig. 10(G)]. Again, frequency dependent attenuation is likely at play here. Larger scale variables have a greater affect at lower frequencies and the  $L_{90}$  NatMin5km [Fig. 10(H),  $L_{50}$  similar] shows that an area must be completely free of unnatural conditions to remain noise free. Regardless of the condition of the majority of an area, the minimum naturalness has a dominant effect affirming that quiet areas require a large buffer. Although anthropogenic sources contribute heavily to the soundscape below 1 kHz, transient events can have impacts at high frequencies over a wide area as shown by the  $L_{10}$  dependence on NatMax5km [Fig. 10(I)]. Low importance variables have minor effects, not necessarily representing entire sources or propagation effect but perhaps a small frequency niche left out by other variables. Less important variables often have effects confined to a narrow range of their values.

The relationships between these geospatial variables and sound levels are undoubtedly complex, and the random forest model introduces additional complications. RANDOM FOREST will seize upon any consistent relationship between the independent and dependent variables, so if the causal input variable is inefficient or not available, the effect of that factor may be attributed to another correlated variable. However, as the soundscape is a collection of many independent sounds that add incoherently, partial dependence functions are appropriate to describe the mix of geospatial features that combine additively and result in predicted spectrum. For example, the soundscape in Fig. 9(A) contains many sources including vehicle traffic, heavy equipment shipping operations, machinery for grounds care, human voices, air traffic, insects, and birdsong, to name a few.

Propagation effects on the other hand, are not necessarily additive. Furthermore, representing and diagnosing the interactive effects of propagation is challenging because attenuation factors are dependent on the path from source to receiver whereas the model framework calculates a homogenous field at each discrete location that is independent of other locations. It is possible that variables disposed to explaining propagation effects could be identified through interaction with source variables. However this is not without uncertainty, for example the effect due to reflection in the ground plane is tied to the landcover variable, which also describes sources. This may be mitigated through inclusion of more propagation-centric variables. Geometric spreading loss, a significant path effect, is accounted for explicitly in some cases by the “distance to” variables such as DistStreamC and DistRoadsMaj.

## V. APPLICATION

This geospatial model can be used to generate predictive maps of sound level variation on landscape and continental

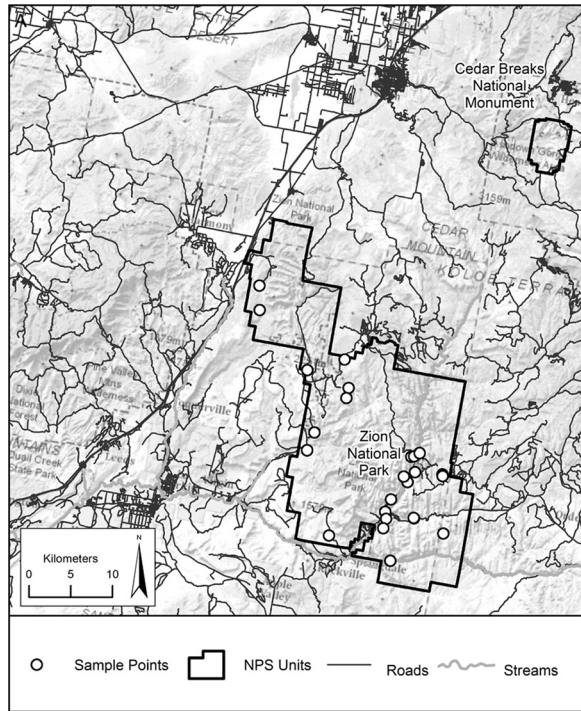


FIG. 11. The study area in southwestern Utah emphasizing some significant geographic features and a subset of the acoustic monitoring sites.

scales, and to evaluate changes in sound levels that would occur under alternative scenarios. To demonstrate this application, a  $69 \times 64$  km rectangle was defined in southwestern Utah containing Zion National Park, Cedar Breaks National Monument, and the nearby towns of Hurricane and Cedar City. Figure 11 shows the study area and some important geographic features including roads, streams, and major terrain features. Explanatory variables were generated at a resolution of 30 m within this study area (4 921 004 point grid). This section focuses on the predictions of four random forest models of the following wideband metrics: the  $A$ -weighted  $L_{10}$ , the unweighted  $L_{10}$ , the  $A$ -weighted  $L_{90}$ , and the unweighted  $L_{90}$ . The performance of these models is itemized in Table II. The contrast between  $A$ -weighted and unweighted sound levels emphasizes spatial changes in low frequency sound levels. Predictions were made independently at each grid point and the resulting maps of the predicted existing sound pressure levels appear in Fig. 12.

The predictions of the  $L_{10}$  exceedance values illustrate the effects of relatively frequent increases in sound level due to transient events. The most prominent features in both the  $A$ -weighted and unweighted plots are elevated levels near the road network, with less marked increases in sound levels associated with river corridors. The  $A$ -weighted plot [Fig. 12(A)] offers a more precise reflection of road and river

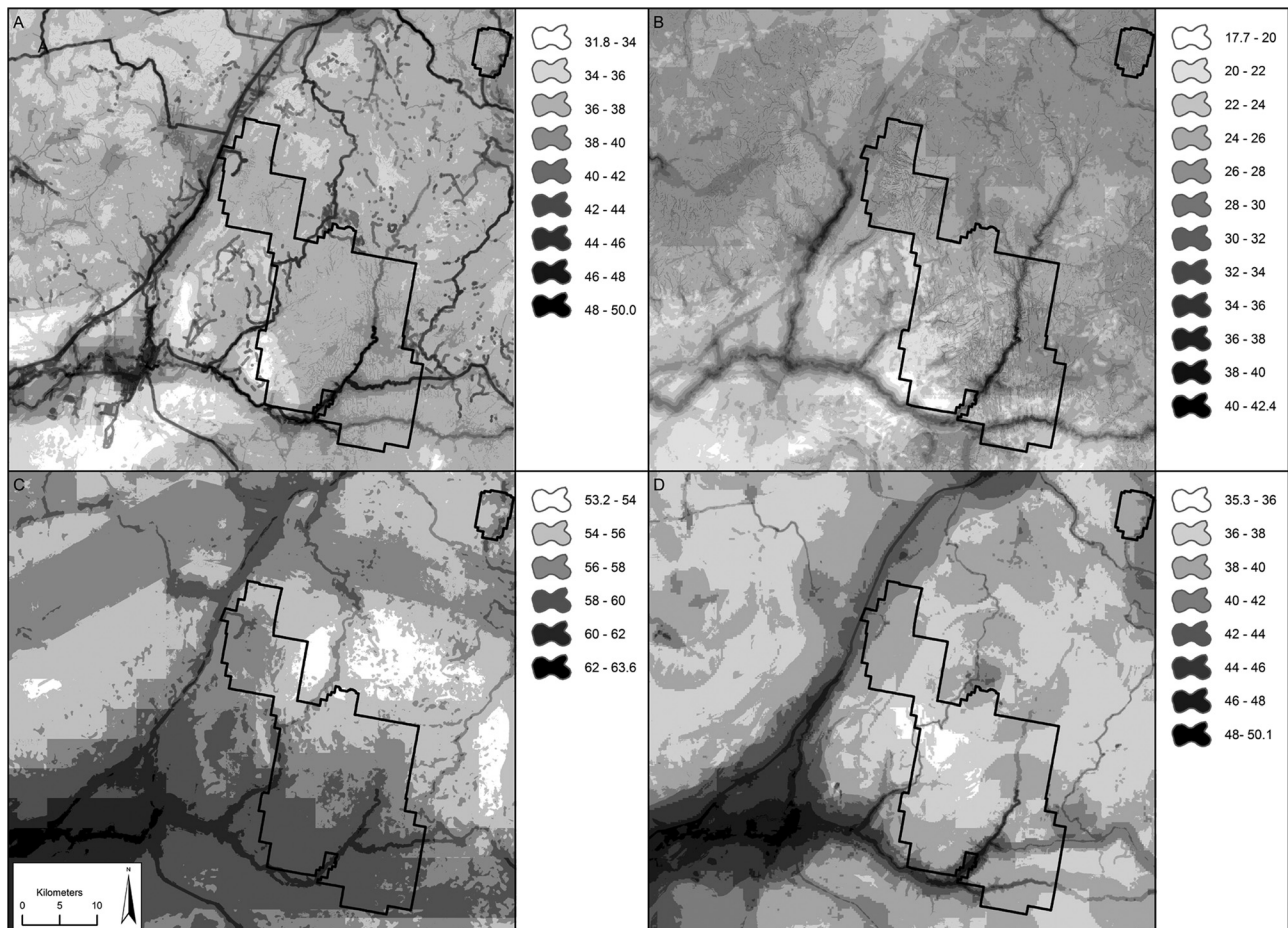


FIG. 12. Predicted existing sound pressure levels across the study area:  $A$ -weighted  $L_{10}$  (A),  $A$ -weighted  $L_{90}$  (B), unweighted  $L_{10}$  (C), and unweighted  $L_{90}$  (D).

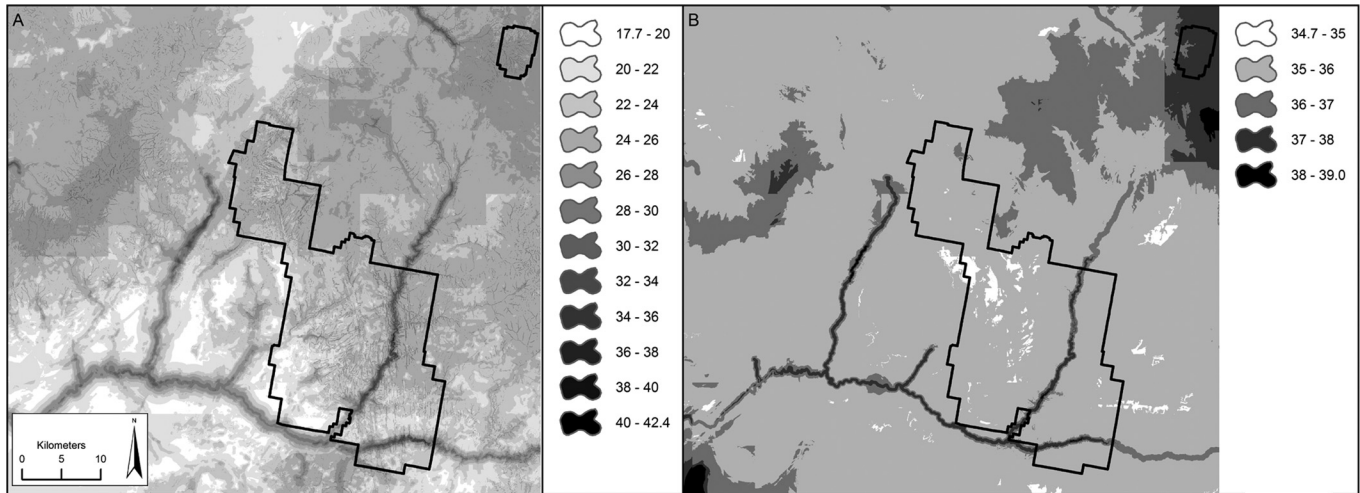


FIG. 13. Predicted sound pressure levels given a natural scenario: A-weighted  $L_{90}$  (A), unweighted  $L_{90}$  (B).

geometry, because the higher frequency sounds emphasized by A-weighting do not propagate as far across the landscape. Note that this propagation effect is not due to explicit physical modeling; it reflects a generic pattern extracted from the measurement sites. The unweighted  $L_{10}$  plot [Fig. 12(C)] also reveals the effect of a military aircraft route that runs through the northern section of the study area. Figures 12(B) and 12(D) displays the same pair of maps for the  $L_{90}$  exceedance value, which represents the background or residual sound level against which other sounds are heard. Developed areas dominate the unweighted map, which adds up to 14 dB in developed areas and along major roads. River corridor and road corridors have roughly equivalent effects in the A-weighted map. This contrast reflects the low-frequency emphasis of road noise.

Maps can also be generated to represent the consequences of changing geospatial inputs. The prevalence of anthropogenic effects recommends developing scenarios that predict what sound levels would be in the absence of noise. In this model, natural scenarios were generated by minimizing the anthropogenic drivers and holding all other variables constant. The accuracy of these predictions is limited by the

training data, but many of the NPS sites had very little anthropogenic influence. For example, for the natural scenarios NatMax5km was set to 0.9966357, the maximum value in the training set (1.0 would be completely natural). Another limitation of these predicted natural conditions is our inability to predict what other geospatial variables would change in the absence of the anthropogenic factors. For example, these natural predictions do not replace the developed landcover sites with a presumed natural landcover, they only remove the developed areas from the area of interest calculations.

The maps of A-weighted and unweighted  $L_{90}$  natural sound levels are displayed in Fig. 13. The A-weighted map reveals much more spatial detail, because it emphasizes higher frequency sounds that do not propagate as far across the landscape. The brightest portions of the A-weighted map are associated with streams and valleys. Landcover also influences this map, with the quietest areas being shrubland dominant (the southwest portion, including Hurricane) and the louder areas having a higher proportion of forest cover (primarily evergreen). High levels of precipitation increase levels to the north and west of the park. In the unweighted

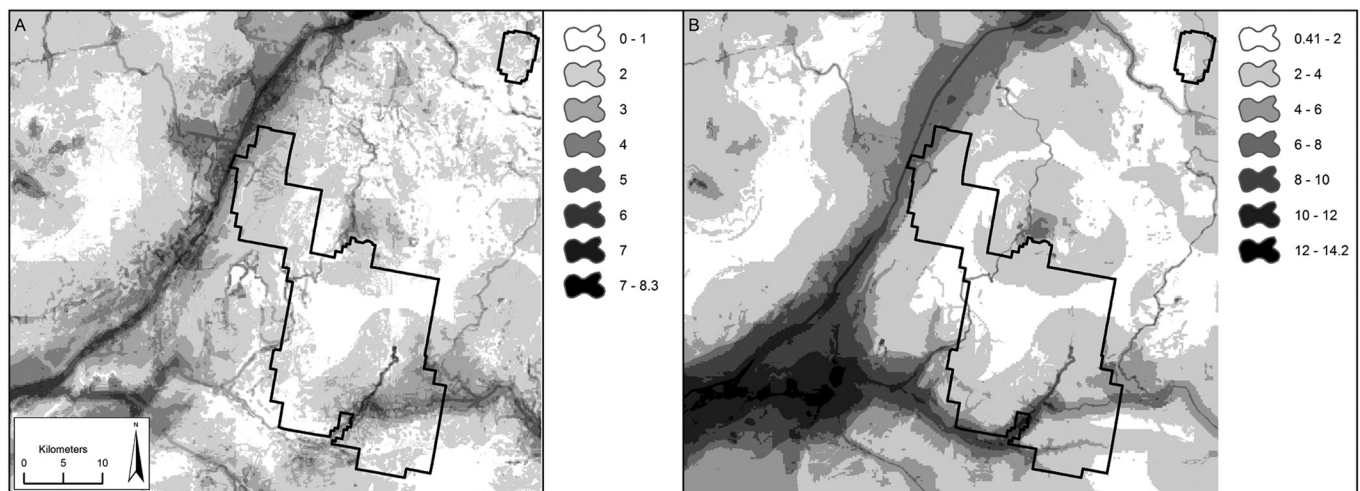


FIG. 14. Predicted impact (dB SPL) of anthropogenic noise on the natural scenario: A-weighted  $L_{90}$  (A), unweighted  $L_{90}$  (B).

map, the illusion of sharp boundaries is an artifact of the very fine gradations in SPL represented by color. Under natural conditions, low frequency sound levels are not predicted to vary much across this landscape.

The net impact of anthropogenic noise can be mapped as the difference between existing and predicted natural sound levels and appear in Fig. 14. These  $L_{90}$  maps document the chronic effects of anthropogenic noise on listening conditions. The *A*-weighted map [Fig. 14(A)] reveals that approximately half of the study area enjoys background sound levels within 1 dB of the natural condition. However, road corridors have extensive spatial influence. Interstate 15 outside the NW edge of Zion elevates background sound levels more than 3 dB far inside the park boundaries. This effect is accentuated in the unweighted map [Fig. 14(B)], which emphasizes the long range effects of low frequency noise. Small changes in  $L_{90}$  translate into substantial effects in auditory awareness. A 3 dB increase in  $L_{90}$  translates to a 50% reduction in listening area for sounds in the same portion of the spectrum as the noise source, and a 6 dB increase translates into a 50% reduction in detection distance.<sup>37</sup>

The example presented here focused on historic, natural conditions. Scenarios can be generated to express potential effects of population growth, energy and transportation development, or the effects of alternative management actions within park boundaries. Geospatial models offer powerful tools for resource stewardship within and well beyond park boundaries.<sup>38,39</sup>

## VI. CONCLUSION

This paper introduced a method to build regression tree-based models that form relationships between measured acoustical data and geospatial data to predict acoustical conditions in environments with an unknown and potentially innumerable amount of acoustic sources and complex, long distance propagation. Through this process, influential covariates of sound pressure levels have been identified and their effects quantified. These results amplify the value of environmental sound level measurements. The National Park Service has invested substantial effort and time to obtain inventories of acoustical conditions across a variety of park unit settings. The geospatial models presented here maximize the spatial applicability of those data by quantifying the relationships between sound level measurements and geospatial data layers that are available for the contiguous 48 states. These models also substantially improve upon the previous treatment of landcover zones as though they had uniform acoustical conditions. These models show that environmental sound levels are a function of multiple factors like landcover, climate, terrain, and even time of year.

These results compliment the established practice of noise propagation modeling. Geospatial models predict sound levels encompassing contributions from all sources, whereas explicit physical models of noise propagation offer powerful tools for predicting the effects of specific noise sources. The spatial resolution and accuracy of noise propagation models can now be complimented by geospatial maps of environmental ambient sound levels, yielding more precise and spatially

extensive prediction of noise to background ratios across landscape scales. For example, the high natural ambient levels caused by wind can be a significant factor in evaluating the potential effects of wind turbine noise.<sup>40</sup>

No physical models of propagation were incorporated in the geospatial model; sound sources were not exhaustively enumerated; source power, spectrum, and directivity were not specified. However, the emergent patterns in the ambient sound level maps are consistent with known properties of environmental sound sources and fundamental principles of acoustic propagation. These physical factors were manifested indirectly. For example, a portion of the higher sound levels near water likely reflects enhanced propagation due to the high acoustic impedance of water. Elevation and TPI are correlated with dissected landscapes where terrain shielding is an important factor. It is striking that the spatial extent of road noise effects displayed in Figs. 12 and 14 are consonant with the spatial extent of noise propagation that would be obtained from physically explicit models like TNM<sup>20</sup> and NMSim.<sup>21</sup>

This paper focused on sound level predictions, but the same approach can be applied to other acoustical metrics like the percent time that noise is audible, and statistics describing the durations of noise-free intervals. Listening to any soundscape, whether at the rim of the Grand Canyon or at a table in a restaurant, is a very rich experience. Several metrics are needed to characterize the diverse dimensions of that experience. These models can also be adapted to look at nocturnal conditions, or even consistent diel patterns.

It might seem reasonable to ask whether there is a great need for geospatial models of acoustical condition. In the United States, noise is arguably one of the fastest growing pollutants.<sup>37</sup> Since 1970, road traffic has tripled and population has increased by a multiple of 1.5. Air traffic, both passenger and freight, has grown faster than surface transportation. Multinational scientific studies of public health and noise have revealed that a significant fraction of the European population is suffering chronic health consequences from noise exposure,<sup>41–43</sup> and the European Union has mandated production of continental scale noise maps.<sup>44,45</sup> The U.S. lags behind Europe in this effort, though exploratory maps of noise exposure have been generated at continental scales.<sup>39,43</sup>

As this paper and other studies document,<sup>4,26,39</sup> noise impacts are not limited to developed areas. Noise is a pervasive threat to ecological integrity and visitor experience in U.S. National Parks and other protected natural areas. One aircraft can broadcast audible noise up to 40 km from its flight path, and a loud truck or motorcycle can cast noise up to 10 km from a road if there is no intervening terrain. Many National Parks enjoy extremely low background sound levels, and like the dim glow of distant lights in a very dark sky, far away noise sources can degrade otherwise outstanding listening conditions for wildlife and park visitors.

<sup>1</sup>N. P. Miller, "US National Parks and management of park soundscapes: A review," *Appl. Acoust.* **69**, 77–92 (2008).

<sup>2</sup>B. C. Pijanowski, A. Farina, S. H. Gage, S. L. Dumyahn, and B. L. Krause, "What is soundscape ecology? An introduction and overview of an emerging new science," *Landscape Ecol.* **26**, 1213–1232 (2011).

- <sup>3</sup>B. De Coensel, D. Botteldooren, and T. De Muer, "1/f noise in rural and urban soundscapes," *Acta Acust. Acust.* **89**, 287–295 (2003).
- <sup>4</sup>E. Lynch, D. Joyce, and K. Fristrup, "An assessment of noise audibility and sound levels in U.S. National Parks," *Landscape Ecol.* **26**, 1297–1309 (2011).
- <sup>5</sup>G. Fleming, C. J. Roof, and D. R. Read, "Draft guidelines for the measurement and assessment of low-level ambient noise," U.S. Department of Transportation report, John A. Volpe National Transportation Systems Center, Acoustics Facility, Cambridge, MA (1998).
- <sup>6</sup>H. Slabbekoorn, "Habitat-dependent ambient noise: Consistent spectral profiles in two African forest types," *J. Acoust. Soc. Am.* **116**, 3727–3733 (2004).
- <sup>7</sup>H. F. Boersma, "Characterization of the natural ambient sound environment: Measurements in open agricultural grassland," *J. Acoust. Soc. Am.* **101**, 2104–2110 (1997).
- <sup>8</sup>O. Fégeant, "Wind-induced vegetation noise. Part 1: A predictive model," *Acta Acust.* **85**, 228–240 (1999).
- <sup>9</sup>O. Fégeant, "Wind-induced vegetation noise. Part 2: Field Measurements," *Acta Acust.* **85**, 241–249 (1999).
- <sup>10</sup>K. Bolin, "Prediction method for wind-induced vegetation noise," *Acta Acust. Acust.* **95**, 607–619 (2009).
- <sup>11</sup>L. N. Miller, "Sound levels of rain and wind in the trees," *Noise Control Eng. J.* **11**, 101–115 (1978).
- <sup>12</sup>S. Morgan and R. Raspet, "Investigation of the mechanisms of low-frequency wind noise generation outdoors," *J. Acoust. Soc. Am.* **92**, 1180–1183 (1992).
- <sup>13</sup>S. Fidell, M. Sneddon, and L. Silvati, "Predicting sound levels from wind speed in a coniferous forest," *J. Acoust. Soc. Am.* **88**, S74 (1990).
- <sup>14</sup>D. J. Mennitt, "Spatial variation of natural ambient sound pressure levels in Rocky Mountain National Park," *J. Acoust. Soc. Am.* **129**, 2617 (2011).
- <sup>15</sup>C. Carroll, R. F. Noss, P. C. Paquet, and N. H. Schumaker, "Use of population viability analysis and reserve selection algorithms in regional conservation plans," *Ecol. Appl.* **13**, 1773–1789 (2003).
- <sup>16</sup>S. Ferrier, "Mapping spatial pattern in biodiversity for regional conservation planning: Where to from here?" *System. Biol.* **51**, 331–363 (2002).
- <sup>17</sup>L. Breiman, "Random forests," *Mach. Learn.* **45**, 5–32 (2001).
- <sup>18</sup>R. H. Bolt and K. U. Ingard, "System considerations in noise control problems," in *Handbook of Noise Control*, edited by C. M. Harris (McGraw-Hill, New York, 1957), p. 22.
- <sup>19</sup>R. E. Liebich and K. C. Chun, "Comparative review of available computer programs for modeling meteorological and terrain effects on long-range propagation of audible noise," *Annual Meeting and Exhibition of the Air and Waste Management Association*, DOE Report No. CONF-940632-13 (1994).
- <sup>20</sup>J. L. Rochat and G. G. Fleming, "TNM version 2.5 addendum to validation of FHWA's traffic noise model (TNM): Phase 1," Report Nos. FHWA-EP-02-031 Addendum and DOT-VNTSC-FHWA-02-01 Addendum, U.S. Department of Transportation, Volpe National Transportation Systems Center, Acoustics Facility, Cambridge, MA (2004).
- <sup>21</sup>B. Ikelheimer and K. Plotkin, "Noise model simulation (NMSim) user manual," Wyle Laboratories Report No. WR 03 9 (2005).
- <sup>22</sup>H. Iyer, "Determination of adequate measurement periods (temporal sampling)," draft report to Natural Sounds Program, Fort Collins, CO (2005).
- <sup>23</sup>T. F. W. Embleton, "Tutorial on sound propagation outdoors," *J. Acoust. Soc. Am.* **100**, 31–48 (1996).
- <sup>24</sup>K. R. Sherrill, "GIS metrics—Soundscape modeling: Standard operating procedure," Natural Resource Report No. NPS/NRSS/IMD/NRR—2012/596, National Park Service, Fort Collins, CO (2012).
- <sup>25</sup>W. B. Monahan, J. E. Gross, L. K. Svancara, and T. Philippi, "A guide to interpreting NPScape data and analyses," Natural Resource technical Report No. NPS/NRSS/NRTR—2012/578, National Park Service, Fort Collins, CO (2012).
- <sup>26</sup>D. M. Theobald, "Estimating natural landscape changes from 1992 to 2030 in the conterminous US," *Landscape Ecol.* **25**, 999–1011 (2010).
- <sup>27</sup>R. A. Berk, *Statistical Learning from a Regression Perspective* (Springer, New York, 2008), pp. 1–355.
- <sup>28</sup>L. Breiman, J. H. Friedman, R. A. Olshen, and C. J. Stone, *Classification and Regression Trees* (Wadsworth & Brooks/Cole, Monterey, CA, 1984), pp. 1–342.
- <sup>29</sup>L. Breiman, "Bagging Predictors," *Mach. Learn.* **24**, 123–140 (1996).
- <sup>30</sup>A. Liaw and M. Wiener, "Classification and Regression by randomForest," *R News* **2**, 18–22 (2002).
- <sup>31</sup>L. Auret and C. Aldrich, "Interpretation of nonlinear relationships between process variables by use of random forests," *Miner. Eng.* **35**, 27–42 (2012).
- <sup>32</sup>J. K. McKee, P. W. Sciuilli, C. D. Fooce, and T. A. Waite, "Forecasting global biodiversity threats associated with human population growth," *Biol. Cons.* **115**, 161–164 (2004).
- <sup>33</sup>J. W. Bradbury and S. L. Vehrencamp, *Principles of Animal Communication* (Sinauer Associates, Sunderland, MA, 1999), pp. 730–740.
- <sup>34</sup>J. H. Friedman, "Greedy function approximation: A gradient boosting machine," *Ann. Stat.* **29**, 1189–1232 (2001).
- <sup>35</sup>E. T. Nykaza, D. K. Wilson, and A. A. Atchley, "Estimation of outdoor sound fields using interpolation and geostatistical models," *Proceedings of Inter-Noise 2012*, New York, NY (2012).
- <sup>36</sup>K. J. Plotkin, "Review of technical acoustical issues regarding noise measurements in national parks," Wyle Report No. WR 01-20, Arlington, Virginia (2001).
- <sup>37</sup>J. R. Barber, K. R. Crooks, and K. M. Fristrup, "The costs of chronic noise exposure for terrestrial organisms," *Trends Ecol. Evol.* **25**, 180–189 (2010).
- <sup>38</sup>K. R. Sherrill and W. H. Romme, "Spatial variation in postfire cheatgrass: Dinosaur National Monument, USA," *Fire Ecol.* **8**, 38–56 (2012).
- <sup>39</sup>J. R. Barber, C. L. Burdett, S. E. Reed, K. A. Warner, C. Formichella, K. R. Crooks, D. M. Theobald, and K. M. Fristrup, "Anthropogenic noise exposure in protected natural areas: Estimating the scale of ecological consequences," *Landscape Ecol.* **26**, 1281–1295 (2011).
- <sup>40</sup>O. Fégeant, "On the masking of wind turbine noise by ambient noise," *European Wind Energy Conference EWEC'99*, Nice, France (1999), pp. 184–188.
- <sup>41</sup>L. Jarup, W. Babisch, D. Houthuijs, G. Pershagen, K. Katsouyanni, E. Cadum, M. L. Dudley, P. Savigny, I. Seiffert, W. Swart, O. Breugelmans, G. Bluhm, J. Selander, A. Haralabidis, K. Dimakopoulou, P. Sourtzi, M. Velonakis, and F. Vigna-Taglianti, "Hypertension and exposure to noise near airports: The HYENA study," *Env. Health Perspect.* **116**, 329–333 (2008).
- <sup>42</sup>W. Babisch, W. Swart, D. Houthuijs, J. Selander, G. Bluhm, G. Pershagen, K. Dimakopoulou, A. S. Haralabidis, K. Katsouyanni, E. Davou, P. Sourtzi, E. Cadum, F. Vigna-Taglianti, S. Floud, and A. L. Hansell, "Exposure modifiers of the relationships of transportation noise with high blood pressure and noise annoyance," *J. Acoust. Soc. Am.* **132**, 3788–3808 (2012).
- <sup>43</sup>N. P. Miller, "Transportation noise and recreational lands," in *The International Congress and Exposition on Noise Control Engineering*, Dearborn, MI (2002).
- <sup>44</sup>K. Kaliski, E. Duncan, and J. Cowan, "Community and regional noise mapping in the United States," *Sound and Vibration Magazine*, September 2007, pp. 14–17.
- <sup>45</sup>European Parliament, of the Council of 25, Directive 2002/49/EC, June 2002 relating to the assessment and management of environmental noise—Declaration by the Commission in the Conciliation Committee on the Directive relating to the assessment and management of environmental noise.